Unearthing exoplanets

Joel Wallenius

Lund Observatory
Lund University

2012-EXA59

Degree project of 15 higher education credits
January 2012

Lund Observatory
Box 43
SE-221 00 Lund
Sweden

Unearthing exoplanets

Joel Wallenius*
Supervisor: David Hobbs†

05/01/12

Abstract

This is a bachelor thesis bent on introducing the field of exoplanet research. It primarily includes descriptions of the various detection methods, with some detail into how the methods yield parameter estimates by means of least-squares algorithms. The feasibility of combining state-of-the-art astrometric capabilities of Gaia and radial velocity measurements from ground level is briefly discussed also, as it is possibly a promising and cheap way of increasing parameter accuracies.

*Lund University, Lund Observatory, Box 43, SE-221 00 Lund, Sweden.
E-mail: joelwallenius@gmail.com
†Lund University, Lund Observatory, Box 43, SE-221 00 Lund, Sweden.
E-mail: david.hobbs@astro.lu.se

Sammanfattning

Den här kandidatuppsatsen skrevs huvudsakligen i syfte att agera språngbräda åt ett mer fördjupande masterprojekt, föreslaget - liksom denna uppsats - av David Hobbs. Den inleder med introduktion och detaljerad härledning av grundläggande omloppsmekanik för gravitationellt bundna system, med utgång från Newtons naturlagar. Detta omfattar t.ex. ellipsformeln, Keplers lagar och andra relevanta samband inklusive radialhastighet. En enkel simulering utförs även här för att visa effekterna av projektion på himlasfären.

Sedan beskrivs i tur och ordning de sex vanligaste metoderna som används för att detektera planeter runt stjärnor utöver Solen. Särskilt fokus har här lagts dels på den metod som nyttjar stjärnors radialhastigheter, och dels på den metod som bygger på astrometri. Astrometrin är måhända särskilt intressant med tanke på att Gaiaexperimentet påbörjas om ett drygt år. Några simulationer av radialhastigheter utförs i tillhörande sektion, om inte annat för att se om den härledda modellen är något att ha.

Därefter beskrivs minsta-kvadratmetoden i syfte att brygga sträckan mellan den praktiska observationen medelst teleskop eller dylikt instrument, och den slutgiltiga uppskattningen av planetsystemens fysikaliska storheter. Majoriteten av - om inte alla - detektionsmetoder inkorporerar minsta-kvadratmetoden på ett eller annat sätt.

Slutligen formuleras ett förslag på hur man kan tänkas kombinera mätdata från radialhastighets- och astrometriexperiment i en gemensam minsta-kvadrat-algoritm, detta i hopp om att förbättra precision och frikoppla parametrar. Denna kombination av mätdata är vad det projekt som denna upptsats agerar språngbräda för ska gå in mer på, är det tänkt.

Uppsatsen avslutas med några tankar om hur framtiden ser ut med avseende på utsikten om att detektera allt mindre och mer jordliknande planeter, något som för många är den heliga graalen inom just detta forskningsområdet.

Contents

1 Introduction

1.1 The ellipse

Johannes Kepler (1571 – 1630) was the first scientist to observe that planets trace elliptical orbits around the Sun.[1]

Ellipses can be defined as the locus of all points whose distance sum to two fixed points in space is constant. In mathematical terms this can be written as

$$\sqrt{\left(x-\frac{D}{2}\right)^2+y^2}+\sqrt{\left(x+\frac{D}{2}\right)^2+y^2}=L$$

where the two fix points (often called focus points or just foci) are situated in a cartesian coordinate system at $\left(-\frac{D}{2},0\right)$ and $\left(\frac{D}{2},0\right)$, and the distance sum is labeled L. This expression can be massaged in simple ways and rewritten into

$$\left(x+\frac{D}{2}\right)^2+y^2=L^2-2L\cdot\sqrt{\left(x-\frac{D}{2}\right)^2+y^2}+\left(x-\frac{D}{2}\right)^2+y^2$$

$$\Leftrightarrow\ x^2+xD+\frac{D^2}{4}=L^2-2L\cdot\sqrt{\left(x-\frac{D}{2}\right)^2+y^2}+x^2-xD+\frac{D^2}{4}$$

$$\Leftrightarrow\ 2xD=L^2-2L\cdot\sqrt{\left(x-\frac{D}{2}\right)^2+y^2}$$

$$\Leftrightarrow\ \frac{L^4-4xDL^2+4x^2D^2}{4L^2}=x^2-xD+\frac{D^2}{4}+y^2$$

$$\Leftrightarrow\ x^2-\frac{x^2D^2}{L^2}+y^2=\frac{L^2-D^2}{4}$$

$$\Leftrightarrow\ x^2\frac{4}{L^2}+y^2\frac{4}{L^2-D^2}=1 \tag{1.1}$$

A geometrical observation (figure 1) is then required to simplify this further. The semi-major and -minor axes are labeled a and b. From the picture, it is realized that the semi-major axis is by definition equal to $\frac{L}{2}$. Using the pythagorean theorem, the isosceles triangle drawn clearly shows that $b^2=\left(\frac{L}{2}\right)^2-\left(\frac{D}{2}\right)^2=\frac{L^2-D^2}{4}$.

Equation 1.1 can then be simplified into

$$\frac{x^2}{a^2}+\frac{y^2}{b^2}=1 \tag{1.2}$$

[1] Today this has been slightly revised - the entire solar system's centre of mass lies completely stationary in a location in which all orbiting bodies' ellipse foci coincide. It should be mentioned however, that if ignoring perturbations caused by the >1 planets of our solar system, Kepler was not incorrect in this conclusion.

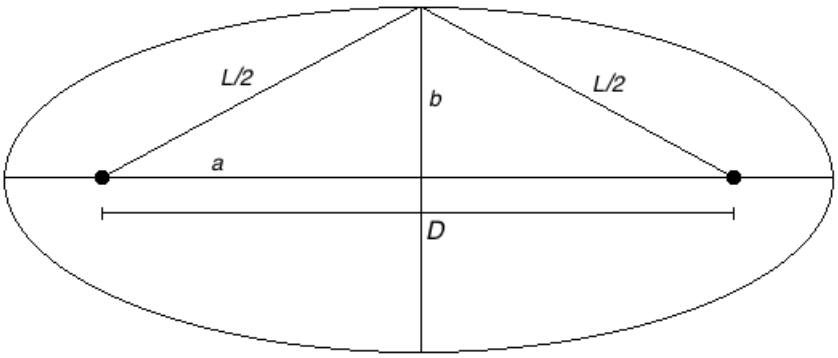

Figure 1: A crudely drawn ellipse with relevant geometry written out.

Eq. 1.2 is the canonical ellipse equation which shows how ellipses differ from circles in a rather intuitive way (margin) - the ellipse can, with some loss of rigour, be thought of as a circle with dimension-specific radii. For the astronomer however, this form is of little or no use. The polar coordinate version with one focus at the origin is better since it expresses the geometry with angles.

$\frac{x^2}{r^2} + \frac{y^2}{r^2} = 1$

If the polar origin is chosen to be the right focus:

$$\frac{\left(x + \frac{D}{2}\right)^2}{a^2} + \frac{y^2}{b^2} = 1$$

By the definition (margin) of eccentricity, e, the shifted canonical equation can be rewritten into:

$e^2 = 1 - \frac{b^2}{a^2}$
$\Rightarrow \frac{D}{2} = ae,$
$\frac{a^2}{b^2} = 1 - e^2$

$$(x + ae)^2 + \frac{y^2}{1 - e^2} = a^2$$

$$\Leftrightarrow\ x^2 + 2aex + a^2e^2 + \frac{y^2}{1 - e^2} = a^2$$

$$\Leftrightarrow\ x^2 + 2aex + \frac{y^2}{1 - e^2} = a^2 - a^2e^2 = a^2\left(1 - e^2\right)$$

$$\Leftrightarrow\ x^2\left(1 - e^2\right) + y^2 = a^2\left(1 - e^2\right)^2 - 2a\left(1 - e^2\right)ex$$

$$\Leftrightarrow\ x^2 + y^2 = a^2\left(1 - e^2\right)^2 - 2a\left(1 - e^2\right)ex + e^2x^2$$

$$\Leftrightarrow\ r^2 = \left[a\left(1 - e^2\right) - ex\right]^2$$

$$\Rightarrow\ r + ex = a\left(1 - e^2\right)$$

$$\Leftrightarrow\ r + er\cos\theta = a\left(1 - e^2\right)$$

$$\Leftrightarrow\ r = \frac{a\left(1 - e^2\right)}{1 + e\cos\theta} \tag{1.3}$$

This is the polar form of conic sections. If e is restricted to $[0, 1)$, this describes an ellipse.

1.2 From Newton to Kepler

Newton's famous law of gravitation may fail at predicting the behaviour of very strong gravitational fields, but it is accurate enough for deriving Kepler's three laws:

1. Planetary orbits are elliptical, with the sun at one focus.
2. The radius vector of the planet orbit sweeps equal areas in equal times (regardless of absolute angular position).
3. The orbital period squared is directly proportional to its semi-major axis cubed.

It so happens that the second law is the most easily derived one, and will therefore be derived first, followed by the first and third.

1.2.1 Kepler's second law

In a polar coordinate system with a star at absolute rest, the orbiting planet position vector will be called $\mathbf{r} = \hat{\mathbf{r}} \cdot r$, where $r = |\mathbf{r}|$, and $\hat{\mathbf{r}}$ then being its unit vector. A second unit vector, $\hat{\theta}$, is directed orthogonally with respect to $\mathbf{r}$, in the approximate direction of planet movement. In order to use Newton's law, the position vector needs to be differentiated with respect to time twice since, according to Newton, any force is $\mathbf{F} = m\ddot{\mathbf{r}} = m\frac{\partial^2(r\hat{\mathbf{r}})}{\partial t^2}$, and the force on the planet would in this case be gravitation:

$$\ddot{\mathbf{r}} = -G\frac{m_{sun} + m_{planet}}{r^2}\hat{\mathbf{r}} \equiv -\frac{\mu}{r^2}\hat{\mathbf{r}} \tag{1.4}$$

Note that the attracting mass is that of the entire system, as opposed to just the star. This is because we've chosen the coordinate origin to be in the star rather than the system's center of mass, but must still account for Newton's third law i.e. that the star should feel the same force as its planet. The acceleration of the star that this necessitates is accounted for by using the system's total mass as the attractor of the planet.

The derivatives of $\mathbf{r}$:

$$\dot{\mathbf{r}} = \frac{\partial\left(\hat{\mathbf{r}}r\right)}{\partial t} = r\dot{\hat{r}} + \hat{\mathbf{r}}\dot{r}$$

Using $\dot{\hat{\mathbf{r}}} = \hat{\theta}\dot{\theta}$, where θ is the polar angle:

$$\dot{\mathbf{r}} = r\hat{\theta}\dot{\theta} + \hat{\mathbf{r}}\dot{r}$$

Now, the second derivative then becomes, with $\dot{\hat{\theta}} = -\hat{\mathbf{r}}\dot{\theta}$:

$$\begin{aligned}\ddot{\mathbf{r}} &= \frac{\partial}{\partial t}\left(r\hat{\theta}\dot{\theta} + \hat{\mathbf{r}}\dot{r}\right) = \frac{\partial}{\partial t}\left(r\hat{\theta}\dot{\theta}\right) + \frac{\partial}{\partial t}\left(\hat{\mathbf{r}}\dot{r}\right) = \dot{\theta}\frac{\partial\left(r\hat{\theta}\right)}{\partial t} + r\hat{\theta}\ddot{\theta} + \dot{r}\dot{\hat{\mathbf{r}}} + \hat{\mathbf{r}}\ddot{r} \\ &= \hat{\theta}\dot{\theta}\dot{r} + r\dot{\theta}\dot{\hat{\theta}} + r\hat{\theta}\ddot{\theta} + \dot{r}\hat{\theta}\dot{\theta} + \hat{\mathbf{r}}\ddot{r} = \hat{\theta}\left(r\ddot{\theta} + 2\dot{\theta}\dot{r}\right) + \hat{\mathbf{r}}\left(\ddot{r} - r\dot{\theta}^2\right)\end{aligned}$$

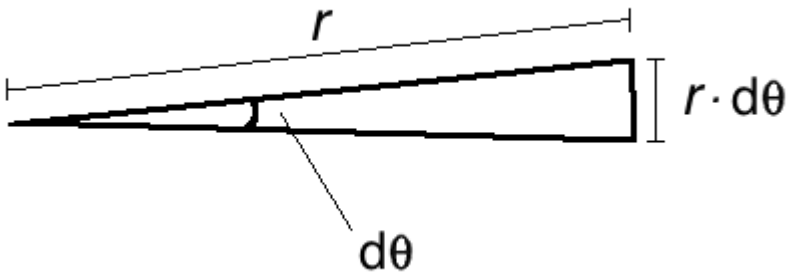

Figure 2: An infinitesimal element of an orbit. The area is that of a triangle, i.e. $r^2 d\theta = r^2 \cdot \dot{\theta} \cdot dt$.

Equating this with 1.4,

$$-\frac{\mu}{r^2}\hat{\mathbf{r}} = \hat{\theta}\left(r\ddot{\theta} + 2\dot{\theta}\dot{r}\right) + \hat{\mathbf{r}}\left(\ddot{r} - r\dot{\theta}^2\right)$$

$$\begin{cases} -\frac{\mu}{r^2} = \ddot{r} - r\dot{\theta}^2 \\ \\ 0 = r\ddot{\theta} + 2\dot{\theta}\dot{r} \end{cases} \tag{1.5}$$

Ignoring the radial result for the moment, the angular result can directly be used to prove Kepler's second law.

The area swept over by the line joining the sun and its planet is $\int \frac{1}{2} r^2 \dot{\theta} dt$, as illustrated by figure 2. The expression $r^2\dot{\theta}$ is constant in time[2], and the integral becomes $\frac{1}{2} r^2 \dot{\theta} \cdot t + C$ which is directly proportional to time. The second law is thus proven, as its statement is equivalent to that swept area is proportional to time.

1.2.2 Kepler's first law

To derive this, it will prove convenient to define $u = \frac{p}{r}$, where $p = \frac{l^2}{\mu}$, with $l = \dot{\theta} r^2$.

To obtain the shape of the orbit, r should be expressed in terms of θ, which can be arranged by differentiating r twice with respect to θ, and then solving the resulting differential equation:

$$\ddot{r} = \frac{\partial \dot{r}}{\partial t} = \frac{\partial}{\partial t}\left(\frac{\partial r}{\partial \theta}\frac{\partial \theta}{\partial t}\right) = \frac{\partial}{\partial t}\left(\frac{\partial r}{\partial \theta}\dot{\theta}\right) = \frac{\partial}{\partial t}\left(\frac{\partial \left(p/u\right)}{\partial \theta}\dot{\theta}\right)$$

[2] $\frac{\partial}{\partial t}\left(r^2\dot{\theta}\right) = \dot{\theta}\frac{\partial r^2}{\partial r}\dot{r} + r^2\ddot{\theta} = r\left(r\ddot{\theta} + 2\dot{r}\dot{\theta}\right) = r \cdot 0 = 0$ Perhaps not-so incidentally, this quantity is the specific angular momentum.

$$= \frac{\partial}{\partial t}\left(\dot{\theta}p\frac{\partial\left(1/u\right)}{\partial\theta} + \frac{\dot{\theta}}{u}\frac{\partial p}{\partial\theta}\right) = ...\left[\frac{\partial p}{\partial\theta} = \frac{1}{\mu}\frac{\partial l^2}{\partial t}\frac{\partial t}{\partial\theta} = 0\right]... = \frac{\partial}{\partial t}\left(-\dot{\theta}pu^{-2}\frac{\partial u}{\partial\theta} + 0\right)$$

$$= -\frac{\partial\left(lp^{-1}\frac{\partial u}{\partial\theta}\right)}{\partial t} = -\frac{\partial\left(lp^{-1}\frac{\partial u}{\partial\theta}\right)}{\partial\theta}\dot{\theta} = -\dot{\theta}\frac{\partial u}{\partial\theta}\frac{\partial\left(lp^{-1}\right)}{\partial\theta} - \frac{\partial^2 u}{\partial\theta^2}\dot{\theta}lp^{-1}$$

$$-\dot{\theta}\frac{\partial u}{\partial\theta}\left(l\frac{\partial\left(1/p\right)}{\partial\theta} + \frac{1}{p}\frac{\partial l}{\partial\theta}\right) - \frac{\partial^2 u}{\partial\theta^2}l^2p^{-3}u^2$$

$$= -\dot{\theta}\frac{\partial u}{\partial\theta}\left(-lp^{-2}\frac{\partial p}{\partial\theta} + \frac{1}{p}\frac{\partial l}{\partial\theta}\right) - \frac{\partial^2 u}{\partial\theta^2}l^2p^{-3}u^2 = -\frac{\partial^2 u}{\partial\theta^2}l^2p^{-3}u^2$$

Inserting this in 1.5, we get

$$-\frac{\mu}{r^2} = -\frac{\partial^2 u}{\partial\theta^2}l^2p^{-3}u^2 - r\dot{\theta}^2$$

$$\Leftrightarrow\ -l^2p^{-3}u^2 = -\frac{\partial^2 u}{\partial\theta^2}l^2p^{-3}u^2 - l^2p^{-3}u^3$$

$$\Leftrightarrow\ -1 = -\frac{\partial^2 u}{\partial\theta^2} - u$$

$$\Leftrightarrow\ \frac{\partial^2 u}{\partial\theta^2} + u = 1$$

One solution to this is $u = 1$, and remaining solutions can be found by adding the solutions of the homogeneous version:

$$\frac{\partial^2 u}{\partial\theta^2} + u = 0$$

The characteristic equation is $R^2+1 = 0$, with solutions $\begin{cases} R_1 = i \\ R_2 = -i \end{cases}$, meaning the general solution is[3]

$$u = C_1\exp\left(i\theta\right) + C_2\exp\left(-i\theta\right)$$

$$= \left(C_1 + C_2\right)\cos\theta + i\left(C_1 - C_2\right)\sin\theta = ...\left[u \text{ is a real quantity}\right]... = e\cos\theta$$

Finally, adding the homogeneous solutions and solving for r:

$$r = \frac{p}{1 + e\cos\theta}$$

This has the same form as the polar form ellipse derived above, and the first law is thus proven.

[3]See any book on differential equations for details of the process. Wikipedia should suffice.

1.2.3 Kepler's third law

The period of an orbit can be expressed as the orbit's area divided by the areal speed:

$$P = \frac{A}{\dot{A}}$$

The area of an ellipse is $\pi ab = \pi a^2\sqrt{1-e^2}$, and the areal speed is $\frac{\dot{\theta}r^2}{2} = \frac{l}{2} = \frac{1}{2}\sqrt{p\mu} = \frac{1}{2}\sqrt{a\left(1-e^2\right)\mu}$:

$$P = \frac{\pi a^2\sqrt{1-e^2}}{\frac{1}{2}\sqrt{a\left(1-e^2\right)\mu}}$$

$$\Leftrightarrow\ P^2 = \frac{4\pi^2 a^4\left(1-e^2\right)}{a\left(1-e^2\right)\mu} = \frac{4\pi^2}{\mu}a^3 \propto a^3 \tag{1.6}$$

$$\Rightarrow\ P^2 \propto a^3$$

The third law is thus proven when assuming a constant μ, which is false for solar systems whose planets are not all perfectly equal in mass. The approximation is good when the planets are light in comparison to their star.

1.3 The ellipse equations

An crucial part of science is gathering information and observing. Unfortunately, exoplanets are presently beyond direct imaging in all but the most extreme cases and their orbital parameters must therefore be deduced indirectly from other, more readily measurable quantities. Some equations that will prove important for this deduction process are:

$$\text{Eccentric anomaly:} \qquad r = a\left(1 - e\cos E\right) \tag{1.7}$$

$$\text{Mean motion:} \qquad n = \frac{2\pi}{P} = \mu^{1/2}a^{-3/2} \tag{1.8}$$

$$\text{Orbital speed:} \qquad V^2 = \mu\left(\frac{2}{r} - \frac{1}{a}\right) \tag{1.9}$$

$$\text{Kepler's equation:} \qquad M = n\left(t - t_p\right) = E - e\sin E \tag{1.10}$$

$$\text{The true and eccentric anomalies:} \qquad \cos\theta = \frac{\cos E - e}{1 - e\cos E} \tag{1.11}$$

$$\text{The 3D-problem:} \qquad \begin{pmatrix} X \\ Y \\ Z \end{pmatrix} = \begin{pmatrix} r\left(\cos\Omega\cos\left(\theta+\omega\right) - \sin\Omega\sin\left(\theta+\omega\right)\cos i\right) \\ r\left(\sin\Omega\cos\left(\theta+\omega\right) + \cos\Omega\sin\left(\theta+\omega\right)\cos i\right) \\ r\sin\left(\theta+\omega\right)\sin i \end{pmatrix} \tag{1.12}$$

$$\text{Radial velocity:} \qquad v_r = V_Z + \frac{na_1\sin i}{\sqrt{1-e^2}}\left(\cos\left(\theta+\omega\right) + e\cos\omega\right) \tag{1.13}$$

Each of these will now be derived and explained.

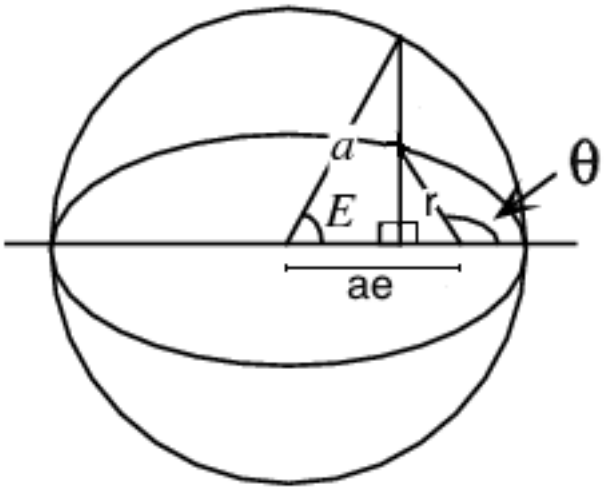

Figure 3: An ellipse and its auxiliary circle, i.e. an overlain circle with a radius equal to the semi-major axis of the ellipse. The angle θ is the true anomaly.

1.3.1 Eccentric anomaly

The so-called eccentric anomaly, E, is the angle depicted in figure 3.

Realized from the geometry:

$$ae = a\cos E + r\cos(\pi - \theta) = a\cos E - r\cos\theta$$

$$\Leftrightarrow \cos\theta = \frac{a(\cos E - e)}{r}$$

$$\Leftrightarrow 1 + e\cos\theta = \frac{ae(\cos E - e) + r}{r}$$

$$\Leftrightarrow \frac{a\left(1-e^2\right)}{1+e\cos\theta} = r = \frac{ra\left(1-e^2\right)}{ae(\cos E - e) + r}$$

$$\Leftrightarrow ae(\cos E - e) + r = a\left(1-e^2\right)$$

$$\Leftrightarrow r = a\left(1-e^2\right) - ae(\cos E - e)$$

$$\Leftrightarrow r = a - ae^2 + ae^2 - ae\cos E$$

$$\Leftrightarrow r = a(1 - e\cos E)$$

With the eccentric anomaly, the rectangular coordinates describing an ellipse can be rewritten:

$$x = a(\cos E - e) \tag{1.14}$$

$$y = a\sqrt{1-e^2}\sin E \tag{1.15}$$

The first equation is obtained by first noting that if we put our origin at the center of the ellipse, then simple geometry gives $x = a\cos E$, and as we switch back to the origin at the right focus, this becomes $x = a\cos E - ae = a(\cos E - e)$.

Again taking the ellipse center as our origin (the y-coordinate does not change!), the second equation can be derived through the canonical ellipse equation:

$$y = b\sqrt{1 - \frac{x^2}{a^2}} = b\sqrt{1 - \frac{a^2\cos^2 E}{a^2}} = b\sqrt{1 - \cos^2 E} = b\sin E = a\sqrt{1 - e^2}\sin E$$

1.3.2 Mean motion

n, sometimes called mean motion, is the lable given to the average angular speed:

$$n = \frac{2\pi}{P}$$

By using 1.6, you immediately get

$$n^2 = \frac{4\pi^2}{P^2} = 4\pi^2\frac{1}{4\pi^2}a^{-3}\mu$$

$$\Rightarrow\ n = a^{-3/2}\mu^{1/2}$$

1.3.3 Orbital speed

The orbital speed V, i.e. the orbit tangent velocity, can be expressed as a function of the orbital separation. To derive it, start with:

$$V^2 = \dot{\mathbf{r}}\cdot\dot{\mathbf{r}} = \frac{\partial(r\hat{\mathbf{r}})}{\partial t}\cdot\frac{\partial(r\hat{\mathbf{r}})}{\partial t} = \left(\frac{\partial r}{\partial t}\hat{\mathbf{r}} + \frac{\partial\hat{\mathbf{r}}}{\partial t}r\right)\cdot\left(\frac{\partial r}{\partial t}\hat{\mathbf{r}} + \frac{\partial\hat{\mathbf{r}}}{\partial t}r\right)$$

$$= \left(\dot{r}\hat{\mathbf{r}} + \dot{\theta}\hat{\theta}r\right)\cdot\left(\dot{r}\hat{\mathbf{r}} + \dot{\theta}\hat{\theta}r\right) = \dot{r}^2 + r^2\dot{\theta}^2$$

To evaluate this, go back to 1.3:

$$\dot{r} = \frac{\partial}{\partial t}\left(\frac{p}{1 + e\cos\theta}\right) = p\dot{\theta}\frac{e\sin\theta}{(1 + e\cos\theta)^2} = \frac{r\dot{\theta}}{1 + e\cos\theta}\,e\sin\theta$$

Now, observe that

$$\frac{r\dot{\theta}}{1 + e\cos\theta} = \frac{l^{1/2}\dot{\theta}^{1/2}}{1 + e\cos\theta} = \frac{p^{1/4}\mu^{1/4}r\dot{\theta}^{1/2}}{p} = p^{-1/2}\mu^{1/2} = \frac{\mu^{1/2}}{a^{1/2}(1 - e^2)^{1/2}} = \frac{na}{\sqrt{1 - e^2}}$$

The expression for $\dot{r}$ then becomes

$$\dot{r} = \frac{na}{\sqrt{1 - e^2}}\,e\sin\theta$$

Using the same observation again,

$$r\dot{\theta} = \frac{na}{\sqrt{1-e^2}}\left(1 + e\cos\theta\right)$$

V^2 can thus be written

$$V^2 = \left(\frac{na}{\sqrt{1-e^2}}\, e\sin\theta\right)^2 + \left(\frac{na}{\sqrt{1-e^2}}\left(1 + e\cos\theta\right)\right)^2$$

$$= \frac{n^2a^2}{1-e^2}\left(e^2\sin^2\theta + 1 + 2e\cos\theta + e^2\cos^2\theta\right) = \frac{n^2a^2}{1-e^2}\left(1 + 2e\cos\theta + e^2\right)$$

$$= \frac{n^2a^2}{1-e^2}\left(2\left(1 + e\cos\theta\right) - \left(1 - e^2\right)\right) = 2n^2a^3\frac{1 + e\cos\theta}{a\left(1-e^2\right)} - n^2a^2$$

$$= n^2a^3\left(\frac{2}{r} - \frac{1}{a}\right) = \mu\left(\frac{2}{r} - \frac{1}{a}\right)$$

$$\therefore V^2 = \mu\left(\frac{2}{r} - \frac{1}{a}\right)$$

1.3.4 Kepler's equation

This derivation begins with $\dot{r}^2 = V^2 - r^2\dot{\theta}^2$, which was shown to be true in the previous derivation. Using the identities found later in that very same derivation, we rewrite into

$$\dot{r}^2 = \mu\left(\frac{2}{r} - \frac{1}{a}\right) - \frac{n^2a^2}{1-e^2}\left(1 + e\cos\theta\right)^2$$

$$\Leftrightarrow \dot{r}^2 = \mu\left(\frac{2}{r} - \frac{1}{a}\right) - n^2a^4\frac{1-e^2}{r^2}$$

$$\Leftrightarrow \dot{r}^2 = \frac{2n^2a^3r}{r^2} - \frac{n^2a^2r^2}{r^2} - \frac{n^2a^4\left(1-e^2\right)}{r^2}$$

$$\Leftrightarrow \dot{r}^2 = \frac{n^2a^2}{r^2}\left(2ar - r^2 - a^2\left(1-e^2\right)\right)$$

$$\Leftrightarrow \dot{r}^2 = \frac{n^2a^2}{r^2}\left(a^2e^2 - \left(r-a\right)^2\right)$$

$$\Leftrightarrow \dot{r} = \frac{na}{r}\sqrt{a^2e^2 - \left(r-a\right)^2}$$

Using the eccentric anomaly identity derived earlier to substitute r:

$$\Leftrightarrow \frac{\partial\left(a - ae\cos E\right)}{\partial t} = \frac{n}{\left(1 - e\cos E\right)}\sqrt{a^2e^2 - \left(a\left(1 - e\cos E\right) - a\right)^2}$$

$$\Leftrightarrow ae\dot{E}\sin E = \frac{n}{\left(1 - e\cos E\right)}\sqrt{a^2e^2\left(1 - \cos^2 E\right)}$$

$$\Leftrightarrow ae\dot{E}\sin E = \frac{nae}{(1 - e\cos E)}\sin E$$

$$\Leftrightarrow \dot{E}\,(1 - e\cos E) = n$$

$$\Leftrightarrow \int \dot{E}\,(1 - e\cos E)\,dt = \int n dt + C$$

$$\Leftrightarrow \int \dot{E} dt - e\int \dot{E}\cos E dt = nt + C$$

$$\Leftrightarrow E - e\int \frac{\partial\,(\sin E)}{\partial t} dt = nt + C$$

Put $C = -nt_p$, where t_p denotes measured time of periapse passage[4]:

$$\Leftrightarrow E - e\sin E = n\,(t - t_p)$$

Now, the *mean anomaly* is defined to be $M = n\,(t - t_p)$, and what do you know - out comes Kepler's equation:

$$M = E - e\sin E$$

1.3.5 The true and eccentric anomalies

This is a simple combination of equations 1.3 and 1.7:

$$r = \frac{a\left(1 - e^2\right)}{1 + e\cos\theta} = a\,(1 - e\cos E)$$

$$\Leftrightarrow \frac{1 - e^2}{1 + e\cos\theta} = 1 - e\cos E$$

$$\Leftrightarrow \frac{1 - e^2}{1 - e\cos E} - \frac{1}{e} = \cos\theta$$

$$\Leftrightarrow \cos\theta = \frac{1 - e^2}{e\,(1 - e\cos E)} - \frac{1 - e\cos E}{e\,(1 - e\cos E)} = \frac{1 - e^2 - 1 + e\cos E}{e\,(1 - e\cos E)} = \frac{\cos E - e}{1 - e\cos E}$$

1.3.6 The 3D-problem

The probability that some planet's orbit is perfectly aligned with the tangent plane of the celestial sphere[5] is zero. A vanishing fraction of systems might have inclinations below measurable values, but the rest will be oriented in all sorts of funny ways. To account for this, a reference coordinate system is introduced. Its axes are labelled X, Y and Z (mutually orthogonal in the usual fashion), where the X and Y-axes are aligned with right ascension and declination respectively (or the other way around depending on preferences), and the Z-axis is pointing to Earth. Its origin coincides with the orbit coordinate system's origin. As

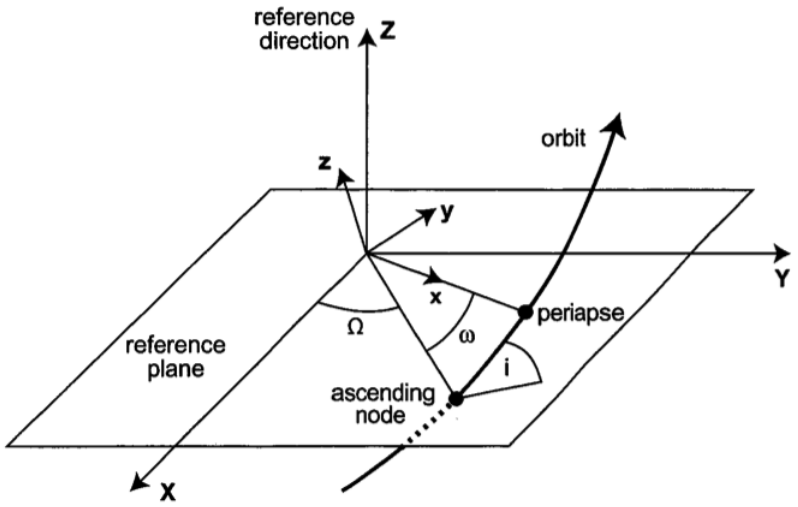

Figure 4: The reference coordinate system XYZ in relation to the orbit coordinate system xyz. The planet orbit is restricted to the xy-plane.

figure 4 demonstrates, the coordinate system of the orbit can be expressed in terms of the reference coordinates by means of three anti-clockwise rotations.

The first rotation is around the z-axis, aligning the x-axis with the line of nodes[6]. The second rotation is around the x-axis, parallelizing the two planes. The third rotation is around the (reoriented!) z-axis, aligning the xy- and XY-planes. These rotations can be mathematically described with 3×3 matrices, since we are dealing with three dimensions.

The standard anti-clockwise rotation matrices are

$$\mathbf{R_x}(\alpha) = \begin{pmatrix} 1 & 0 & 0 \\ 0 & \cos\alpha & -\sin\alpha \\ 0 & \sin\alpha & \cos\alpha \end{pmatrix}$$

$$\mathbf{R_y}(\alpha) = \begin{pmatrix} \cos\alpha & 0 & \sin\alpha \\ 0 & 1 & 0 \\ -\sin\alpha & 0 & \cos\alpha \end{pmatrix}$$

$$\mathbf{R_z}(\alpha) = \begin{pmatrix} \cos\alpha & -\sin\alpha & 0 \\ \sin\alpha & \cos\alpha & 0 \\ 0 & 0 & 1 \end{pmatrix}$$

[4] I.e. time of minimum distance from the planet's star.

[5] An imaginary and arbitrarily distant sphere centered on Earth upon which objects in the sky may be projected for geometrical convenience.

[6] The intersection between the orbital plane and the XY-plane is commonly referred to as the line of nodes.

The subscript denotes which axis the rotation is performed around. Using the notation in figure 4, we can write

$$\begin{pmatrix} X \\ Y \\ Z \end{pmatrix} = \mathbf{R_z}(\Omega)\,\mathbf{R_x}(i)\,\mathbf{R_z}(\omega)\begin{pmatrix} x \\ y \\ z \end{pmatrix} = \mathbf{R_z}(\Omega)\,\mathbf{R_x}(i)\begin{pmatrix} x\cos\omega - y\sin\omega \\ x\sin\omega + y\cos\omega \\ z \end{pmatrix}$$

$$= \mathbf{R_z}(\Omega)\begin{pmatrix} x\cos\omega - y\sin\omega \\ \cos i\,(x\sin\omega + y\cos\omega) - z\sin i \\ \sin i\,(x\sin\omega + y\cos\omega) + z\cos i \end{pmatrix} =$$

$$= \begin{pmatrix} \cos\Omega\,(x\cos\omega - y\sin\omega) - \sin\Omega\,(\cos i\,(x\sin\omega + y\cos\omega) - z\sin i) \\ \sin\Omega\,(x\cos\omega - y\sin\omega) + \cos\Omega\,(\cos i\,(x\sin\omega + y\cos\omega) - z\sin i) \\ \sin i\,(x\sin\omega + y\cos\omega) + z\cos i \end{pmatrix}$$

$$= \begin{pmatrix} r\,(\cos\Omega\cos(\theta+\omega) - \sin\Omega\sin(\theta+\omega)\cos i) \\ r\,(\sin\Omega\cos(\theta+\omega) + \cos\Omega\sin(\theta+\omega)\cos i) \\ r\sin(\theta+\omega)\sin i \end{pmatrix}$$

The last step is performed by substituting x and y into their polar forms, using trigonometric identities and finally noting that $z = 0$ for all points in the planet orbit. As X, Y, Z and the various angles are measured (if possible), this matrix takes care of the problematic 3D aspects. Figures 5 and 6 showcase the reality of the 3D-problem.

1.3.7 Radial velocity and barycentric motion

This derivation is rather lengthy. For starters, express the position of the system's center of mass $\mathbf{R}$:

$$\mathbf{R} = \frac{\sum m_i r_i}{\sum m_i} \rightarrow \frac{M\mathbf{r}_1 + m\mathbf{r}_2}{M+m}$$

Where $M = m_{star}$, $m = m_{planet}$ and the two vectors $\mathbf{r}_1$ and $\mathbf{r}_2$ are the position vectors of the star and its planet respectively (note that the vector $\mathbf{r}$ used earlier can now be written as $\mathbf{r}_2 - \mathbf{r}_1$).

Now, define two additional vectors $\mathbf{R}_1$ and $\mathbf{R}_2$:

$$\mathbf{R}_1 = \mathbf{r}_1 - \mathbf{R}$$

$$\mathbf{R}_2 = \mathbf{r}_2 - \mathbf{R}$$

This definition implies that

$$M\mathbf{R}_1 + m\mathbf{R}_2 = M\,(\mathbf{r}_1 - \mathbf{R}) + m\,(\mathbf{r}_2 - \mathbf{R}) = M\mathbf{r}_1 + m\mathbf{r}_2 - \mathbf{R}\,(M+m)$$

$$= \mathbf{R}\,(M+m) - \mathbf{R}\,(M+m) = 0$$

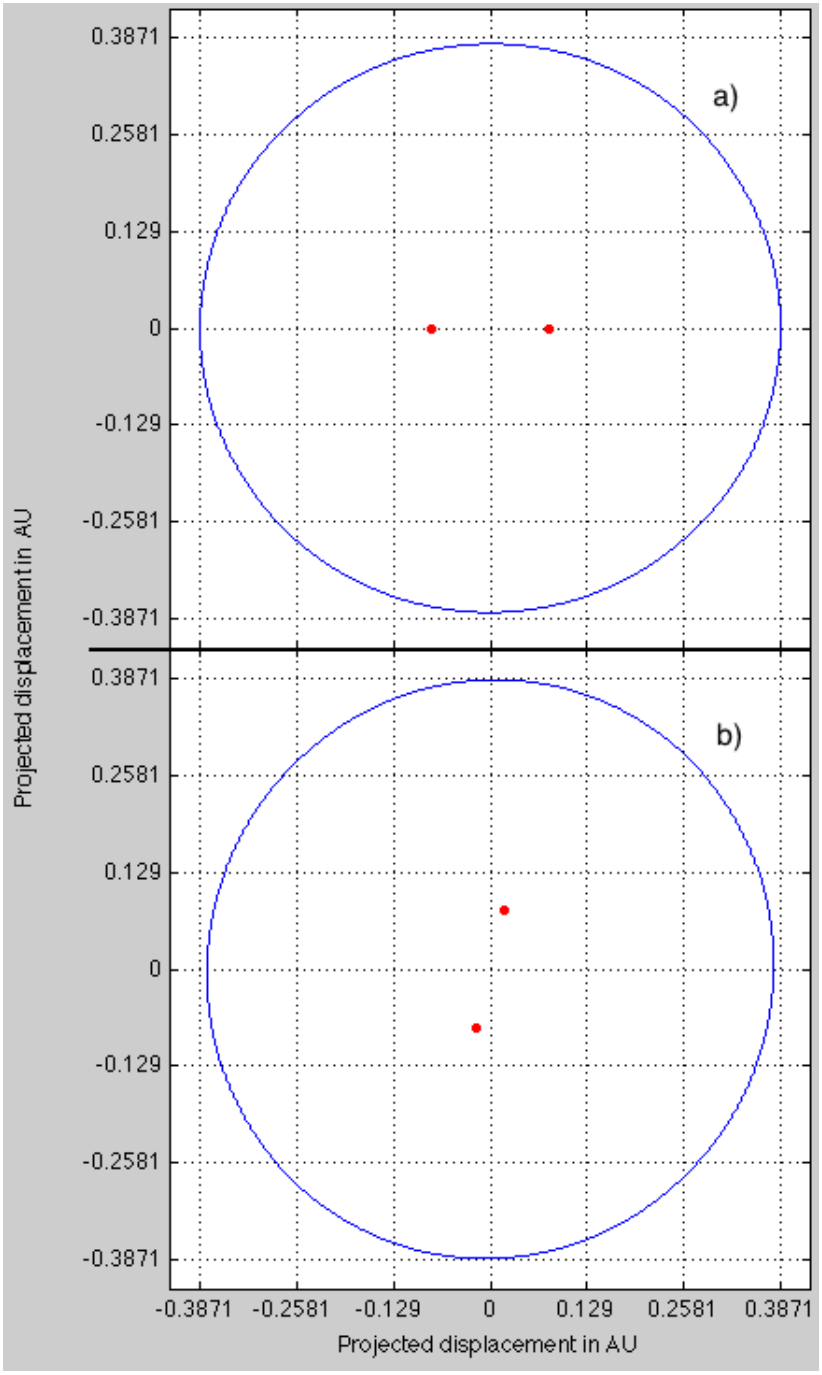

Figure 5: The orbit of Mercury observed a) head-on and b) from a direction perpendicular to the solar system invariable plane, with the vernal equinox pointing to the right. The red points are the orbit foci, of which one is the position of the Sun, and the other is imaginary.

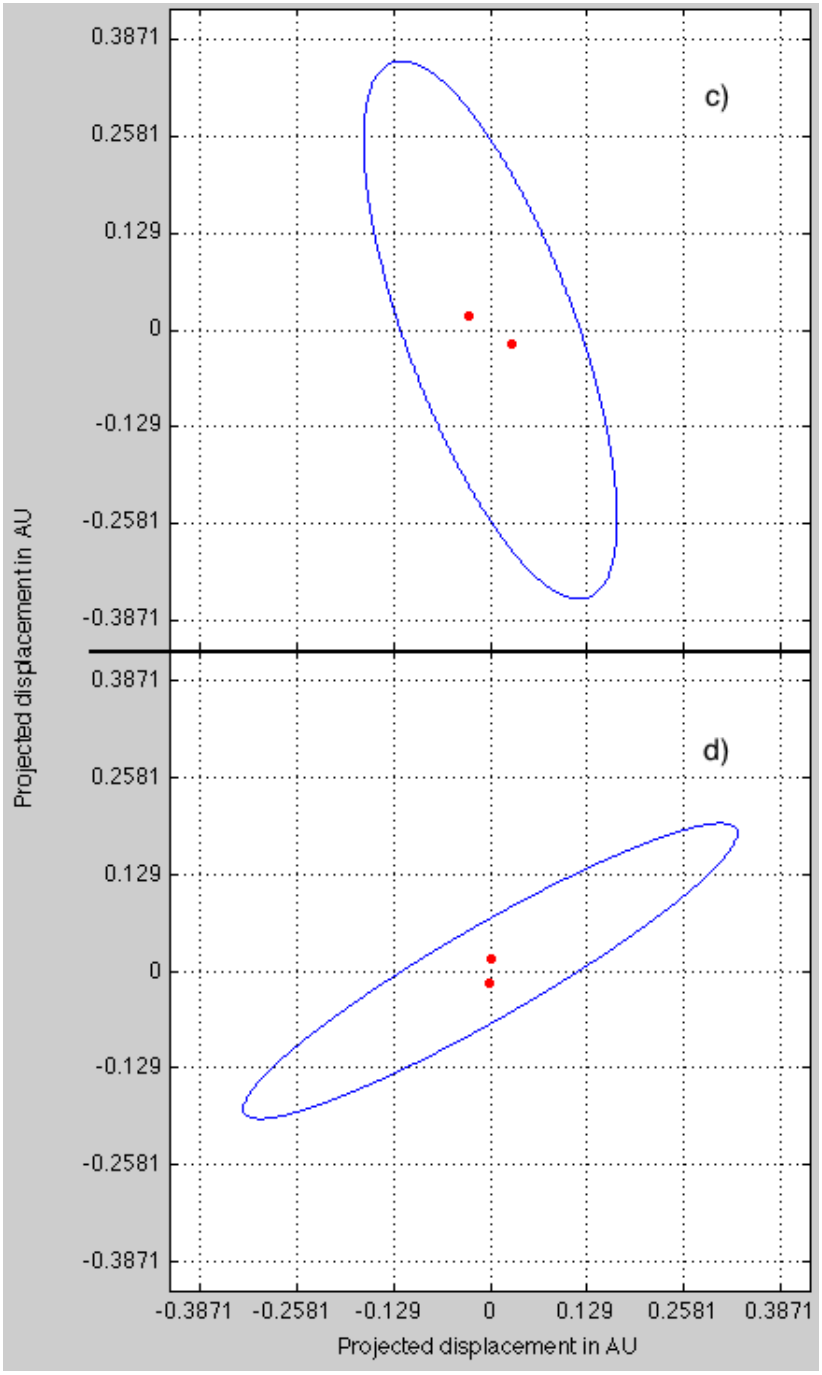

Figure 6: The orbit of Mercury observed from some two random positions (vernal equinox pointing wherever). Note how the difference in foci orientation from c) to d) is important to avoid false impressions of elliptical orbit shapes.

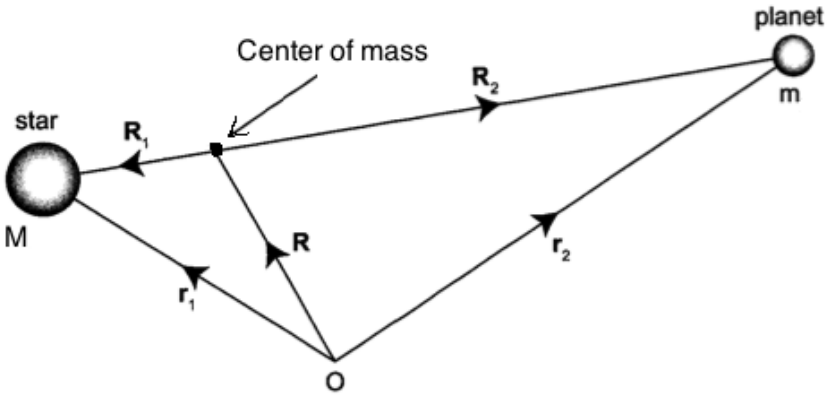

Figure 7: A planet and its star with relevant position vectors drawn with respect to origin O.

As $\mathbf{R}_1$ and $\mathbf{R}_2$ have opposite directions, the magnitudes must then obey:

$$MR_1 = mR_2$$

Now, with assistance from figure 7, observe how

$$r = |\mathbf{r}_1 - \mathbf{r}_2| = |\mathbf{R}_1 - \mathbf{R}_2| = R_1 + R_2$$

The two last equations can be combined:

$$\begin{aligned} R_1 = \frac{m}{M}(r - R_1) = \frac{m}{M}r - \frac{m}{M}R_1 \\ \Leftrightarrow R_1\left(1 + \frac{m}{M}\right) = \frac{m}{M}r \\ \Leftrightarrow R_1 = \frac{{}^{m}/_{M}}{\left(\frac{M+m}{M}\right)}r = \frac{m}{M+m}r \end{aligned} \tag{1.16}$$

In the same manner,

$$R_2 = \frac{M}{M+m}r$$

Applying eq.1.3 to this finding gives:

$$R_1 = \frac{ma}{M+m}\frac{\left(1-e^2\right)}{1+e\cos\theta} = a_1\frac{\left(1-e^2\right)}{1+e\cos\theta}$$

$$R_2 = \frac{Ma}{M+m}\frac{\left(1-e^2\right)}{1+e\cos\theta} = a_2\frac{\left(1-e^2\right)}{1+e\cos\theta}$$

Spelling it out, the star and its planet will trace elliptical orbits around the center of mass, and their eccentricities will be equal to each other and to the eccentricity of the planet-star orbit. The differences arise as a scaled major axis, as the equations demonstrate.

As for the radial velocity, the various vectors defined can now be collectively massaged into an expression for either the star's or the planet's velocity along the Z-axis. As Doppler spectroscopy allows us to measure the radial velocity of the star, this quantity is the more important one for the time being. Start by projecting star velocity on the Z-axis (now originating from the center of mass!) and take it from there:

$$v_r = \dot{\mathbf{r}}_1 \cdot \hat{Z} = \frac{\partial \left(\mathbf{R} + \mathbf{R}_1\right)}{\partial t} \cdot \hat{Z} = \dot{\mathbf{R}} \cdot \hat{Z} + \dot{\mathbf{R}}_1 \cdot \hat{Z} = V_Z + \dot{Z}$$

$$\dot{Z} = \sin i \left(R_1 \dot{\theta} \cos\left(\theta + \omega\right) + \dot{R}_1 \sin\left(\theta + \omega\right) \right)$$

Use the identities for $\dot{r}$ and $r\dot{\theta}$ found in the derivation of Kepler's equation:

$$\dot{Z} = K \left(\cos\left(\theta + \omega\right) + e \left(\sin\theta \sin\left(\theta + \omega\right) + \cos\theta \cos\left(\theta + \omega\right) \right) \right)$$

$$= K \left(\cos\left(\theta + \omega\right) + e \left(\cos\omega \left(\sin^2\theta + \cos^2\theta \right) + \sin\theta \cos\theta \sin\omega - \cos\theta \sin\theta \sin\omega \right) \right)$$

$$= K \left(\cos\left(\theta + \omega\right) + e\cos\omega \right) = \frac{n a_1 \sin i}{\sqrt{1 - e^2}} \left(\cos\left(\theta + \omega\right) + e\cos\omega \right)$$

$$\therefore v_r = V_Z + \frac{n a_1 \sin i}{\sqrt{1 - e^2}} \left(\cos\left(\theta + \omega\right) + e\cos\omega \right)$$

The constant $K = \frac{n a_1 \sin i}{\sqrt{1-e^2}}$ is introduced to simplify what meets the eye but also represents an amplitude of sorts, as the only other factor in the expression is periodic. V_Z is the projected systemic velocity, i.e. the center-of-mass velocity in the radial direction.

2 Methods of detection

Exoplanets are intrinsically elusive from our perspective on Earth. To the best of our knowledge, their vast majority exists only as companions of stars (the minority being Rogue planets), and as they neither fuse their own nuclear fuels or reflect isotropically without losses, light signals from exoplanets are effectively drenched in their parent star's brilliance. This poses a problem with observations as long as our instruments are not adequately sensitive or resolving (they pretty much are not, as of today). There are however a number of circumstances which present possibilities – both for direct and indirect observations.

2.0.8 Rogue planets

Planets are not necessarily orbiting their parent stars. During star system formation, they could conceivably be thrown out by some unfortunate instability, drifting for ages through interstellar space. Alternatively, the gas cloud collapse mechanism that is believed to account for the existence of stars could also result in less massive bodies, reminiscent of Jovian planets.

Detecting these planets is obviously a great challenge, since their Planck radiation is weak. Apart from direct imaging, the only conceivable method for detection is gravitational lensing. As explained below however, this technique suffers from the requirement of chance alignments on the celestial sphere, and is therefore largely unable to bear appreciable fruit.

2.1 Radial velocity

As a planet and its star orbit their common center of mass, the star will from Earth appear to move along a more or less inclined ellipse. The radial component of movement will cause a slight Doppler shift of the star's spectrum, which a sufficiently sensitive spectrograph could measure. Today, velocity variations over 1 m/s are measurable. Successful use of this technique gives a minimum mass of the exoplanet or the true mass if the inclination of the orbital plane happens to be known. An example of a situation where the inclination is known would be that of simultaneous applications of the transit method (explained later) and this spectroscopy method – for starters, observable transits always imply inclinations $\sim 90°$, but the transit method can on its own constrain this value further. This is of great help of course, since the $\sin i$ factor would cease to be a problem.

Problems with this technique include minute inclinations and sluggish orbital periods – a planet orbiting its star in a plane perpendicular to our line of sight will yield a radial velocity of zero, and orbital periods of tens or hundreds of years might not disclose adequate velocity changes during the experiment lifetime.

How does one extract velocity from the measured Doppler shift? Start with the relativistic expression:

$$\lambda_{obs} = \lambda_{em} \frac{1 + \beta \cos \alpha}{\sqrt{1 - \beta^2}}$$

As per standard notation, $\beta = {}^{v}/_{c}$. The factor $\cos \alpha$ accounts for the fact that it's the projected velocity along the line of sight that matters (incidentally a classical approximation). As star system velocities are on the order of 100 km s^{-1}, $\beta^2 \sim 10^{-12} \approx 0$, we can approximate into

$$\lambda_{obs} = \lambda_{em} \left(1 + \beta \cos \alpha\right) = \lambda_{em} + \lambda_{em} \frac{v \cdot \cos \alpha}{c}$$

$$\Leftrightarrow v \cdot \cos \alpha = \frac{\lambda_{obs} - \lambda_{em}}{\lambda_{em}} c$$

$$\Leftrightarrow v_r = \frac{\Delta\lambda}{\lambda_{em}} c$$

As mentioned above, the radial velocity method gives a minimum mass estimate of the exoplanet. How? Massage the expression for K with Kepler's third law:

$$K = n\frac{\sin i}{\sqrt{1-e^2}} a_1 = \frac{2\pi}{P}\frac{\sin i}{\sqrt{1-e^2}}\left(\frac{P^2 G M_*}{4\pi^2}\right)^{1/3} = \frac{\sin i}{\sqrt{1-e^2}}\left(\frac{2\pi G M_*}{P}\right)^{1/3}$$

$$= \left(\frac{2\pi G}{P\left(1-e^2\right)^{3/2}}\right)^{1/3} M_*^{1/3} \sin i = \left(\frac{2\pi G}{P\left(1-e^2\right)^{3/2}}\right)^{1/3} \frac{m \sin i}{\left(M+m\right)^{2/3}}$$

... where M_* is the equivalent attracting mass in the COM-star system.

Under the assumption that the planet mass is very minute in relation to its star's, and that the star mass can be estimated with the theory of stellar structure and evolution (e.g. using temperature and luminosity), K can be simplified into

$$K = \left(\frac{2\pi G}{P M^2 \left(1-e^2\right)^{3/2}}\right)^{1/3} m \sin i$$

... where everything inside the paranthesis is available. Sadly this is as far as it gets if using the radial velocity method alone.

2.1.1 Complications

When measuring in practise, the V_Z term in the radial velocity equation is measured from our own solar system's center of mass. From there, one must of course take into account the velocity of the spectrometer used, along with a problematic bunch of various velocity sources:

- Earth motion and rotation, including perturbations caused by the rest of the solar system. Today, proper adjustments for these effects can bring the introduced error below 1 m s^{-1}.
- Stellar motion in the galaxy, i.e. projection effects. Nearby stars can have significant acclerations in the radial direction if the projection geometry is changing rapidly. Barnard's star for example appears to accelerate radially at 4.50 m s^{-1} yr^{-1} .
- Stellar rotation, convection granules and star spots. The effects of these phenomena vary between minute to about 1 km s^{-1}.
- Gravitational distortion of space-time. These values are typically on the order of several hundreds of m s^{-1}. Lower for red giants, higher for white dwarves.

With all these nuisances in mind, it is no small challenge to measure radial velocity wobbles caused by exoplanets at workable signal-to-noise ratios. Earth's influence on the sun (when observing in the ecliptic) is for example about 0.1 m s^{-1}:

$$\left(\frac{2\pi G}{PM^2\left(1-e^2\right)^{3/2}}\right)^{1/3} m\sin i = \left(\frac{2\pi G}{PM^2}\right)^{1/3} m = \left(\frac{2\pi G}{PM^2}\right)^{1/3} m =$$

$$= \left(\frac{2\pi \cdot 6.67384\cdot 10^{-11}\mathrm{N}(m/kg)}{365.256363004...\text{ days}\cdot\left(1.9891\cdot 10^{30}\right)^2\mathrm{kg}^2}\right)^{1/3} 5.9736{\cdot}10^{24}\text{ kg} = 0.089...\text{ m s}^{-1}$$

2.1.2 Finding parameters

So let's say the astronomer has measured the wobble of some star with sufficient resolution. How do you go about translating the data points into a model? The answer is for the majority of astronomers a non-linear least-squares algorithm, whereby you input an initial guess of each of the parameters (e.g. period, eccentricity etc.), and the algorithm will iteratively change the values a bit back and forth until the model fits optimally to the data points acquired through measurement. For the algorithm to function, the partial derivatives of the model with respect to each of its parameters need to be supplied. According to Wright & Howard (2009), these derivates are:

$$\frac{dE}{dP} = \frac{{}^{-2\pi(t-t_p)}/_{P^2}}{1-e\cos E}$$

$$\frac{dE}{dt_p} = \frac{{}^{-2\pi}/_{P}}{1-e\cos E}$$

$$\frac{dE}{de} = \frac{\sin E}{1-e\cos E}$$

$$\frac{\partial\theta}{\partial E} = \sqrt{\frac{1+e}{1-e}}\frac{1+\cos\theta}{1+\cos E}$$

$$\frac{\partial\theta}{\partial e} = \frac{\partial\theta}{\partial E}\frac{\sin E}{1-e^2}.$$

At first glance these derivatives do not appear to tie any strings together, considering the appearance of the model (eq. 1.13). For the purposes of mathematical (at the expense of conceptual) simplicity and numerical efficiency, Wright & Howard rewrite the model into

$$v_r = h\cos\theta + c\sin\theta + v_0$$

where the three introduced parameters are defined as

$$h = K\cos\omega$$

$$c = -K \sin \omega$$

and

$$v_0 = V_Z + Ke \cos \omega.$$

Writing v_r as the scalar product between its parameters and the independent variable, i.e. $v_r = \vec{\beta}\mathbf{F} = \begin{pmatrix} h & c & v_0 \end{pmatrix} \begin{pmatrix} \cos\theta \\ \sin\theta \\ 1 \end{pmatrix}$, the derivative can be written

$$\frac{dv_r}{dx} = \frac{d\left(\vec{\beta}\mathbf{F}\right)}{dx} = \frac{d\vec{\beta}}{dx}\mathbf{F} + \frac{d\mathbf{F}}{dx}\vec{\beta},$$

where x denotes any of the parameters that $\mathbf{F}$ is a function of. $\frac{d\mathbf{F}}{dx}$ can be evaluated by using Kepler's equation and eq. 1.11, and it just so happens[7] that $\frac{d\vec{\beta}}{dx}$ as well can be expressed in terms of $\frac{d\mathbf{F}}{dx}$, reducing the problem to calculating the inner derivatives of $\mathbf{F}$, i.e. the derivatives of the true anomaly, which in turn can be expressed as[8]

$$\frac{d\theta}{dx} = \frac{\partial\theta}{\partial x} + \frac{\partial\theta}{\partial E}\frac{dE}{dx}.$$

From this vantage point, the derivatives above tie together the loose ends. For a contextual perspective, read the section below on the least-squares algorithm.

2.1.3 Simulations

Simulated plots of radial velocity are displayed in figures 8 and 9. Parameters for the simulations were collected from Wikipedia (the solar system planets) and exoplanets.org (HD 4113). Date of collection was 29/12/2011.

2.2 Planet transits

If fortune smiles upon the observing astronomer, an exoplanet's orbit is nearly perpendicular to the plane of the sky. Then, every time the planet passes in front of its star it will occlude it slightly – the planet's dark disk replaces a fraction of the star's shining disk. As is the case for most detection techniques, multiple planets will reveal themselves through the superposition of their individual effects - in this case, a periodic modulation of apparent star luminosity.

To see if this technique is practically feasible, an example calculation could be performed. Let's say Jupiter passes in front of the sun at a distance great enough to regard the two bodies as two-dimensional. Jupiter's radius is roughly a tenth of the sun's, and since disk area scales with radius squared, the Sun would appear to lose about 1 % of its luminosity. This is not impossible to measure since it happens to correspond to a magnitude change of about 0.01,

[7] For details on this refer to their paper.
[8] Again, refer to the original paper for details.

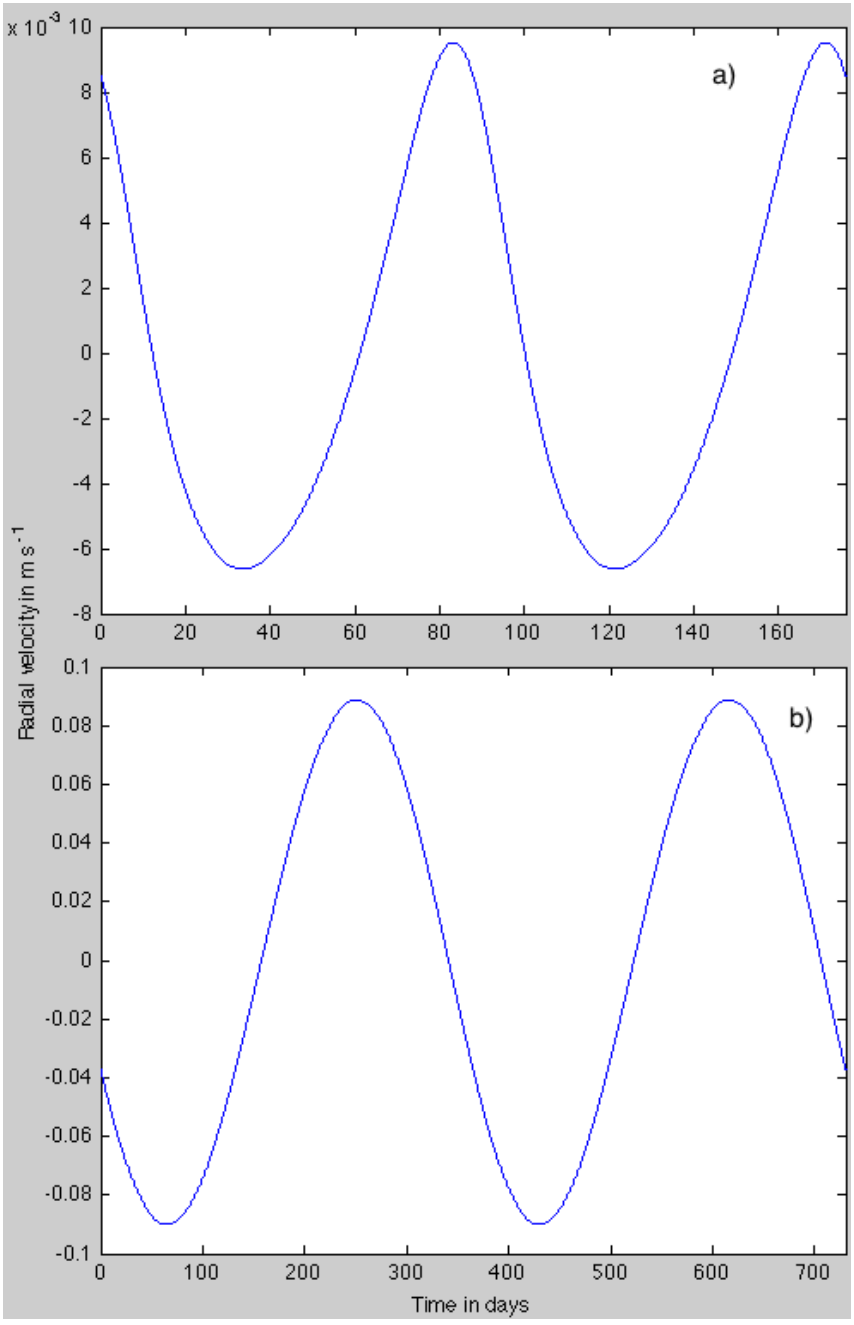

Figure 8: The simulated reflex wobble of the sun from a) Mercury and b) the Earth. The observer is situated in the solar system's invariable plane, moving with the solar system barycentre and having the vernal equinox as reference direction. Time is measured from moment of perihelion passage, and is not mutual. Note the shifting axis scales.

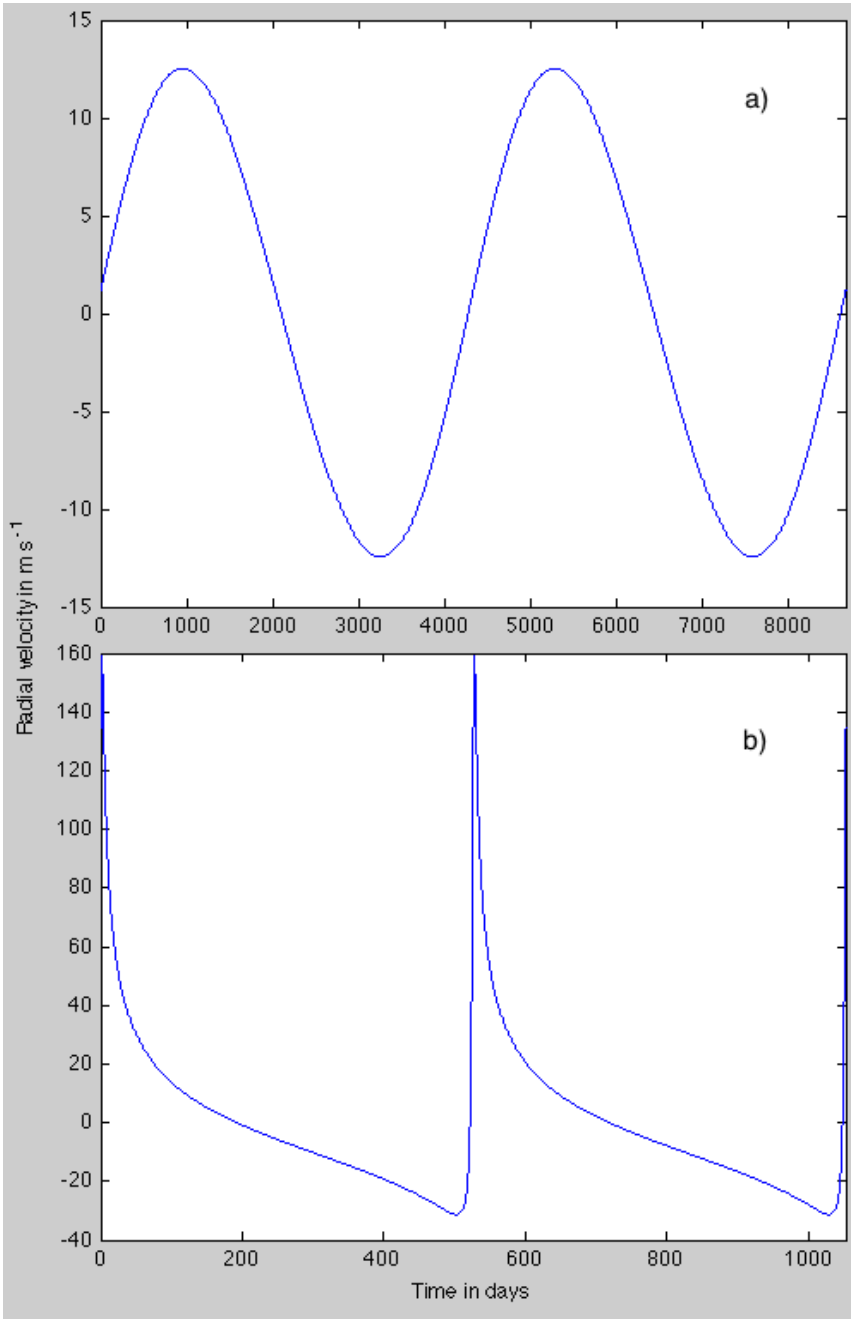

Figure 9: The simulated reflex wobble of a) the sun from Jupiter and b) HD 4113 from HD 4113b. In a) the observer is situated in the solar system's invariable plane. The vernal equinox is used as reference direction. Systemic velocities have been removed. Time is measured from moment of perihelion passage, and is not mutual. Note the shifting axis scales.

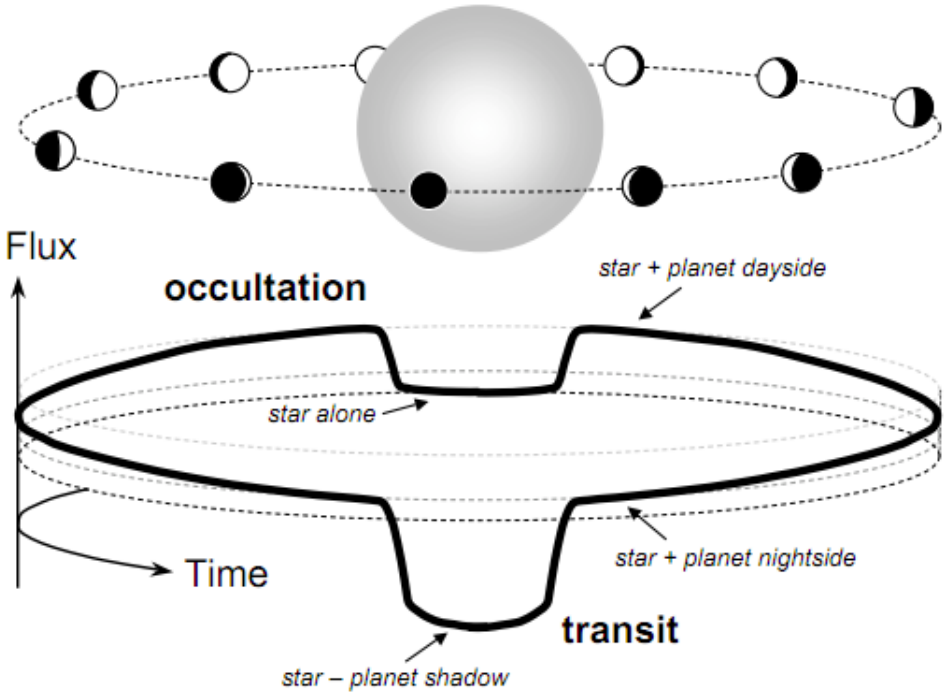

Figure 10: A basic schematic of what the transit method offers. The dashed lines in the picture's lower half indicate levels of same flux. Figure taken from Winn (2010).

and that is a precision often found in tables of star magnitudes. For the time being, ground-based telescopes do not much surpass this precision, while space-based telescopes tend to be a rough order of magnitude or so more precise, corresponding to the ability to find planets a few times more massive than Earth. This technique benefits from short periods (increases probability of detection and improves signal-to-noise ratio) and sizeable planets (stronger occlusion), with fortunate alignment obviously being a prerequisite.

As can be seen in figure 10, a property of the transit method that emerged during the past decade is exploitation of the fact that bodies around stars go through phases (they reflect different amounts of starlight depending on the observer's perspective) just like our own moon. This particular part of the transit technique is applicable on any orbit inclination, but is a rather weak method on its own as it requires higher photometric sensitivity.

2.2.1 From observables to model parameters

The directly measurable quantities from observing a periodically occluding system are

1. *Transit depth* $\frac{\Delta F}{F}$, where F represents flux in some way. ΔF is defined as the difference between the flux received immediately before the transit initiates, and the flux received at maximum occlusion.

2. Period P, obviously. Unless the planet orbit precesses excessively, measuring the period is quite straightforward.

3. *Total transit duration* τ_T, i.e. the time elapsed between the two instants determined by the planet touching the rim of the stellar disk on its way over, and then having just left it.

4. τ_F, i.e. the time elapsed while the planet disk is completely within the stellar disk.

All four of these are directly available from a data series of flux vs time. Periodograms[9] could be employed for data extraction. The transit method can however give us much more under certain assumptions and the theoretical models constructed from those assumptions. It might be tempting to use a simple model wherein two spheres gradually overlap in a circular orbit, but as is often the case, reality is more complicated than that.

Limb darkening

The photosphere of stars have finite opacity and negative temperature/density gradients (diminishes towards surface). This means that one will observe higher blackbody temperature i.e. higher photon flux when the line of sight is parallell to the star's surface normal, and lower flux as the angle between line of sight and surface normal increases. This obviously has an effect on the transit light curve since the planet will, as it moves across the stellar disk, occlude areas of varying brightness - the sometimes smoothed edges of transit curves, including rounded shapes of the primary transits, are because of limb darkening. To make matters worse, limb darkening is a function of the wavelength band observed in. Longer wavelengths tend to give less pronounced limb darkening, while shorter wavelengths have the opposite effect. For models on limb darkening, see Mandel & Agol (2002) and Seager & Mallén-Ornelas (2003).

Eccentricitiy

Circular orbits would be neat, but from radial velocity measurements we know that 25 % or so of transiting planets have significant eccentricities. The effects of this include but might not be restricted to asymmetry in the light curve, a bias in transit probability and total transit duration. The curve asymmetry can be quantified by noting the difference between the durations of a transit's ingress and egress. Barnes (2007) derived an expression for the duration of either one:

$$\tau = \frac{R_p\sqrt{1-e^2}}{v_0\left(1+e\cos\theta\right)\cos\left(\arcsin b\right)},$$

[9] A representation of the data in frequency space, obtained through the Fourier transform.

where R_p is the planet's radius, v_0 is the azimuthal velocity (velocity component perpendicular to direction of orbit curve) for a circular orbit with the same semi-major axis as the actual planet and b is the planet's impact parameter with respect to the star. The difference will be non-zero for all eccentric systems whose argument of pericentre or apocentre do not happen to coincide with the mid-transit position.

The transit probability for highly eccentric orbits is actually higher than for low eccentricities. This is because, while for a planet the time spent close (close as in closer than semi-major axis) to its star is independent of its eccentricity, the angular portion of its orbit spent close to its star increases with eccentricity. Planets closer to their stars produce a larger solid angle wherein the transit is visible due to elementary projection geometry. If then two planets have different eccentricities but equal semi-major axes, the planet with the higher eccentricity will spend a larger fraction of its orbit at a distance shorter than the semi-major axis. Figure 11 demonstrates this. It follows that eccentricity will produce a bias in transiting systems, and the 25 % of transiting planets found to be significantly eccentric are not representable for the entire population. See Kipping (2008) and Barnes (2007) for models taking the eccentricity into account.

Reflected light

This was mentioned earlier - given a planet with non-zero albedo (i.e, it does not absorb all incoming radiation), the starlight reflected upon its surface is detectable in principle. In fact, secondary transits (planet transit on the far side of its star as seen from Earth) imply its existence - if the planet was completely dark, there would not be any secondary transits. A complication though this might be, it is actually rather fortunate as it allows the use of more detailed models and thus the prospect of estimating additional parameters.

According to Collier Cameron et al. (1999) and Leigh et al. (2003a), the flux ratio ϵ between the planet's reflected starlight and the star's normal output can be written

$$\epsilon = p\left(\lambda\right)\left(\frac{R_p}{a}\right)^2 g\left(\alpha\right),$$

where $p\left(\lambda\right)$ is the brightness ratio between the planet at zero phase (entire hemisphere irradiated) and a Lambertian flat disk, $g\left(\alpha\right)$ is the phase function which describes how the reflected starlight's projection is modulated in the orbit and a is the semi-major axis of the planet orbit.

As is often praxis, the various parameters in the many models are estimated through least-squares fitting.

2.2.2 Polarimetry and spectroscopy

Starlight from sunlike stars is largely unpolarized on the whole, but varies between stellar limb and center. This presents two oppurtunities - if the starlight exhibits excessive and time-varying polarization, this is indicative of an exoplanet presence since its atmosphere reflects and polarizes during its phases,

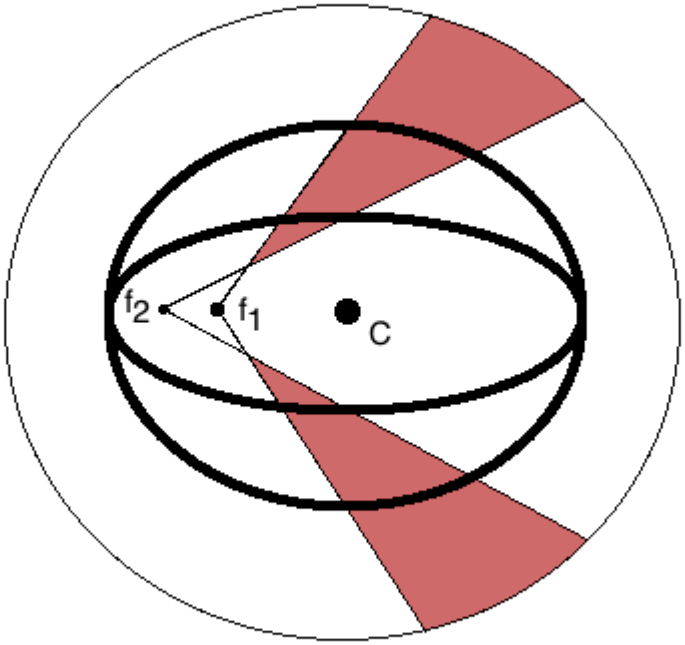

Figure 11: Two planet orbits showing why planets in eccentric orbits are easier to spot with the transit method. The shaded region illustrates the extra angles spent at a distance shorter than the common semi-major axis, if your planet orbits around f_2 with higher eccentricity rather than f_1 with lower eccentricity. The larger circle represents the celestial sphere, with C being the geometrical center for all three ellipsoids.

while if an exoplanet transits the star and thus occludes areas on the stellar disk of varying degrees of polarization, this would also betray the planet's existence (Leroy, 2000). The latter of these effects may suffice for detecting Earth-like planets, and estimating the orbit eccentricity (Carciofi & Magalhães, 2005), while the former could potentially allow estimation of P, e, and i, but also give hints about the nature of the particles in the atmosphere responsible for the scattering process.

Polarization is not the only effect that atmospheres of exoplanets contribute with, they also constitute a source of absorption and/or emission lines in the integrated system spectrum. The absorption is relevant when the planet passes in front of the star, as a fraction of the starlight is then forced to pass through the exoplanet atmosphere. As this happens, the primary transit depth will vary slightly as a function of the wavelength observed with because matter does not generally absorb light uniformly over the EM spectrum. The projected area of the exoplanet atmosphere during full transit is, depending on the geomtrical shape of the planet, an annulus with a radial dimension of something like $5 \cdot H$ where the canonical scale height H is:

$$H = \frac{kT}{\mu_m g_p},$$

with k being Boltzmanns constant, T the temperature, $\mu_m$the mean molecular mass (of the absorbing particles) and g_p the surface gravity on the exoplanet. Expressed with H, the area ratio (serving as an estimation of the absorbed flux fraction) between the atmosphere annulus and the stellar disk is on the order of $\sim 10\frac{R_p H}{R_*^2}$ where R_p and R_* is the planet radius and the stellar radius respectively. As an example, the atmosphere of a Jupiter-sized planet orbiting very close to its star (i.e. a 'Hot Jupiter') would absorb around 10^{-4} of the starlight. Note that, unfortunately, the absorption scales with the inverse of molecular mass, and eventual organic i.e. heavy molecules will not assist this technique (Seager et al., 2009).

The emission on the other hand is observable by calculating the spectrum difference between star plus planet and star alone (secondary transit), or star plus planet and star minus planet (primary transit). Either way will estimate the spectrum of the planet. This spectrum supplies information on e.g. temperature gradients in the planet's atmosphere (emission lines would indicate a positive gradient for example), element abundances, albedo etc.

2.3 Timing

The period of a signal from an accelerating system will appear to change in time in all cases except for when the signal is emitted from an object in circular orbit around the observer (ignoring relativistic effects). In astrophysics, these systems are not uncommon. Examples include pulsars, eclipsing binaries and pulsating stars. This technique is powerful because the complex physical situation boils down to very accurate timekeeping - something we're rather good at. As a

testament to this, the lowest-mass exoplanet discovered as of 2010 (named PSR B1257+12 A) was found around a millisecond pulsar with a mass of 0.02 Earths.

2.3.1 Pulsar timing

Pulsars are neutron stars[10] whose radio emission beams coincidentally sweep across Earth. If they are not undergoing dynamical changes (for example, accreting mass from a companion), their rotation periods are practically constant - they typically slow down at 10^{-15} seconds per revolution, corresponding to 0.03 seconds in a million years. This is quite fortunate, as it gives the astronomer a chance to detect very minute accelerations of the neutron star. How? If a planet is orbiting the pulsar, this implies a reflex wobble i.e. periodic velocity modulation. If for example the pulsar is wobbling away form Earth at increasing radial velocity, and during that time sends two signals, the second signal will be sent at a slightly greater distance than it would if the pulsar was moving with constant velocity, and the period will appear to have increased since the speed of light is finite. Without knowing the radial velocity of the pulsar, its absolute period is not available, but this does not affect the applicability of the technique.

An obvious downside to using pulsars is their rarity (total number confirmed is currently approaching 2000), but one could also question the usefulness in searching for planets around pulsars when remembering how neutron stars are formed (supernova explosions). Granted, theories of dynamic nature would not mind, while the astrobiologist would. It is a bit sad that the best instrument available to us for detecting planets of earthlike mass is unavailable up until the point where potential life as we know it is wiped clean from the system.

2.3.2 Eclipsing binaries

Timing can also be applied on binary star systems with inclinations minute enough for eclipsing to occur. As the two stars revolve, their brightness signal will change periodically as they align themselves with Earth. An exoplanet in orbit around them both will cause their mutual center of mass to wobble, and as was the case for pulsars, this will yield a modulation of the signal period.

The signal period for eclipsing binaries is generally a lot longer than it is for pulsars. This means rather large errors in the period measurements, and consequently difficulties with estimating modulations of the period. In order to penetrate the noise, the modulation must be significant i.e. the orbiting planet should be massive, it should be orbiting at a large distance, and for statistical purposes its period should be short (short period implies higher number of measurements). These terms are not satisified simultaneously, since Keplerian orbits link orbit distance with orbit period (eq 1.6). As an example, Wolszczan derived an equation in 1997 that implies detectability of planets at about ten Jupiter masses, given a timing accuracy on the binary period of 10 s and planet orbit periods of 10-20 years.

[10]The remains of stars who were of roughly 8 - 40 solar masses.

2.3.3 Pulsating stars

Detecting and characterising planets around stars in advanced stages of evolution is interesting because it would supply us with information on planet survivability under dynamically violent circumstances, and thus how our own solar system might look like in the coming billions of years. Presently, the vast majority of pulsating stars under investigation (for purposes of detecting exoplanets) are white dwarves. As they cool down, their surface atmospheres are ionized in various ways, creating density gradients and displacements of these. As gravity tends the system to equilibrium, positional oscillations of the atmosphere arise. These periods typically take on values between 100 and 1000 seconds, and are actually remarkably stable and thus excellent clocks.

The periods are not as impressive as those found with pulsars, and consequently the lowest mass of an orbiting body needed for detectability is a lot higher. On the other hand, white dwarves are fairly common in the solar neighbourhood, much unlike pulsars.

2.4 Astrometry

Remembering equation 1.16, the projected semi-major axis of a star in a solar system (the *astrometric signature*) is

$$\alpha = \frac{a^*}{d} \sin i = \frac{m}{M} \frac{a}{d} \sin i, \tag{2.1}$$

where a^* and a are the semi-major axes of the star perturbing planet respectively, d is the distance to the star from Earth, i is the inclination, m is the planet mass and M is the star mass.

As is obvious from this equation, the star's wobble on the celestial sphere is most easily measured when a number of fortunate circumstances are present. The inclination should ideally be around 90 degrees, the orbiting planet should be massive and at a respectable orbit distance while the system should not be too far off from Earth. This contrasts with the preferred circumstances in using radial velocity or transits where you would desire short orbital periods and minute inclinations, which implies that the techniques are somewhat complementary. The GAIA and SIM[11] -missions will pioneer the search for exoplanets with astrometry – progenitor instruments have simply not been sensitive enough, and as α scales reciprocally with distance, there will be issues even for future missions beyond a certain parallax.

Astrometry might seem deceptively straightforward when regarding equation 2.1, but is unfortunately very much not so. As the instrument accuracy creeps down towards the venerable 1 μas, various physical effects will have a significant impact on the measurement. These effects include:

- Aberration. The tangential velocity of an observer relative to the object being observed will shift the apparent source position towards the apex of

[11] Actually SIM has been cancelled, but luckily chinese astronomers are aiming to undertake a very similar mission based on SIM, so hopefully the essence of the mission is not lost.

the observer velocity, since the speed of light is finite. Abberation will shift star positions by about 20 as, depending on where in its elliptical orbit Earth happens to be. Modern models of relativity are powerful enough to sufficiently account for this effect.

- Gravitational distortion of space-time. The gravitational potential well of our sun will deflect incoming light to some extent, shifting apparent star positions away from the sun with a few mas, with differential values (i.e. those which will show when measuring wobble) of about 1 μas, depending primarily on the star's apparent position, its wobble and the angle between source direction and the ecliptic. Best case is of course when this angle is zero, assuming the sun's gravitational field is spherically symmetric. As is the case for aberration, the relativity models available today are more than enough to compensate for this at μas accuracy.

- Stellar motion in the galaxy. The Milky Way is spinning, but not particularly uniformly with respect to its inhabitant stars. Stellar velocities will appear to change in all sorts of ways with the projection geometry, yielding so-called *perspective acceleration.* These effects are particularly significant at small distances, which is unfortunate as shorter distances generally means data which is both more accesible and more precise.

- Stellar surface structure jitter and disk instabilities. Sunspots and other exotic phenomena may very well shift the photocentre of a star, while gravitational instabilities in the circumstellar disk may cause slow but significant and unpredictable reflex motions.

2.4.1 Modeling

For the purpose of including the influence of exoplanets in the astrometrical model, we describe the stellar motion on the celestial sphere using rectangular coordinates for their conceptual simplicity. Remember eq 1.12? If one would reverse the polar form and ignore the Z-component (astrometry is only rarely capable of measuring it anyway), you get, after some rearranging:

$$\begin{pmatrix} X \\ Y \end{pmatrix} = \begin{pmatrix} x\left(\cos\Omega\cos\omega - \sin\Omega\sin\omega\cos i\right) + y\left(-\cos\Omega\sin\omega - \sin\Omega\cos\omega\cos i\right) \\ x\left(\sin\Omega\cos\omega + \cos\Omega\sin\omega\cos i\right) + y\left(-\sin\Omega\sin\omega + \cos\Omega\cos\omega\cos i\right) \end{pmatrix}$$

From here, we define for convenience a handful of constants[12]:

$$A = a^*\left(\cos\omega\cos\Omega - \sin\omega\sin\Omega\cos i\right)$$

$$B = a^*\left(\cos\omega\sin\Omega + \sin\omega\cos\Omega\cos i\right)$$

$$F = a^*\left(-\sin\omega\cos\Omega - \cos\omega\sin\Omega\cos i\right)$$

$$G = a^*\left(-\sin\omega\sin\Omega + \cos\omega\cos\Omega\cos i\right)$$

[12]Often referred to as Thiele-Innes constants, although their appearance can differ subtly from author to author.

Now, the long matrix equation above can be neatly condensed into

$$X = Ax + Fy \tag{2.2}$$

$$Y = Bx + Gy. \tag{2.3}$$

Note that this definition of X and Y requires a normalisation of the coordinates x and y (compare with equations 1.14 and 1.15):

$$x = \cos E - e$$

$$y = \sqrt{1 - e^2} \sin E$$

Accounting for nominal star position (α_0, δ_0) at $t = t_0$, parallax ϖ, proper motion (μ_α, μ_δ), ignoring the various error sources described above, the astrometric position $(\alpha(t), \delta(t))$ of a star at a time t can now be written, after introducing the planet-induced wobble from eqs 2.2 and 2.3:

$$\alpha(t) \cos\delta = \alpha_0 \cos\delta + \varpi \Pi_{\alpha,t} + \mu_\alpha \cos\delta (t - t_0) + Bx(t) + Gy(t)$$

$$\delta(t) = \delta_0 + \varpi \Pi_{\delta,t} + \mu_\delta (t - t_0) + Ax(t) + Fy(t)$$

The funny-looking $\Pi_{\alpha,t}$ and $\Pi_{\delta,t}$ are the so-called *parallax* factors, accounting for Earth's elliptical motion around the sun[13].

The model is now ready as input for a least-squares algorithm. This necessitates finding the model's partial derivatives with respect to all the various unknown parameters. Wright & Howard (2009) undertook and completed this quest:

$$\frac{dx}{dP} = -\frac{dE}{dP} \sin E$$

$$\frac{dx}{dt_p} = -\frac{dE}{dt_p} \sin E$$

$$\frac{dx}{de} = -\frac{dE}{de} \sin E - 1$$

$$\frac{dy}{dP} = \sqrt{1 - e^2} \cos E \frac{dE}{dP}$$

$$\frac{dy}{dt_p} = \sqrt{1 - e^2} \cos E \frac{dE}{dt_p}$$

$$\frac{dy}{de} = \sqrt{1 - e^2} \cos E \frac{dE}{de} - \frac{e \sin E}{\sqrt{1 - e^2}}$$

The various derivatives of the eccentric anomaly were expressed earlier in section 2.1.

Now what? See the section below on the least-squares algorithm.

[13] For more on this see the papers by Green in 1985 and Seidelmann in 1992.

2.5 Gravitational microlensing

Gravitational lensing is a phenomenon predicted in general relativity, and it has been observed on multiple occasions. The principle is such that any lump of matter will bend the geometry of space-time in its vicinity towards itself, implying amongst other things that straight lines cease to be straight and that light rays passing by massive objects are focused to significant degrees. Application of this phenomenon in the search for exoplanets is possible if Earth and two stars happen to be aligned along a straight line. The closer star will then deflect and focus the photons of the farther star. As this happens, assuming the closer star happens to host a planet, that planet's own gravitational field will superpose a weak lensing effect over its star's.

When observing these lensing effects as a consequence of galaxies and galaxy clusters, the lens and the possibly several distorted images it produces are generally resolvable. Obviously and unfortunately, stars and planets are not as big as galaxies and as long as we are unable to resolve them, the lensing effect will manifest only as a characteristic and sudden increase in apparent flux from the farther star.[14] In this flux modulation, there will be introduced irregularities as a consequence of the asymmetrical mass distribution of planetary systems (unless of course the asymmetry somehow through the geometrical projection mimics something resembling a point mass e.g. the star on its own), and it is these irregularities that can be translated into physical parameters of the lensing system.

Interesting advantages of this technique include:

- A relatively weak dependency on both distance and planet mass (several kpc or Earth-massed planets respectively is in principle not a problem).
- Complete independency on wavelength (photons of different wavelengths will be affected identically with respect to the gravitational lens).
- Its potential ability to detect rogue planets, and thus extract information on e.g. their frequency.
- Its maximal planet-detection sensitivity at orbital separations of around 1 AU, which translates to the habitable zone for many main sequence stars.

... while not-so-interesting disadvantages include:

- The signifcant rarity of the prerequisite chance alignments. Staring towards the high-density galactic bulge, you can't expect more than $\sim 10^{-8}$ of the stars to undergo a lensing event at any one time that could betray the presence of an exoplanet. Large enough surveys can remedy this to some extent, fortunately.
- The fact that in practise, observations can only be performed once, meaning you don't get second chances.

[14] The unability to resolve the situation is the reason for naming the technique microlensing rather than lensing.

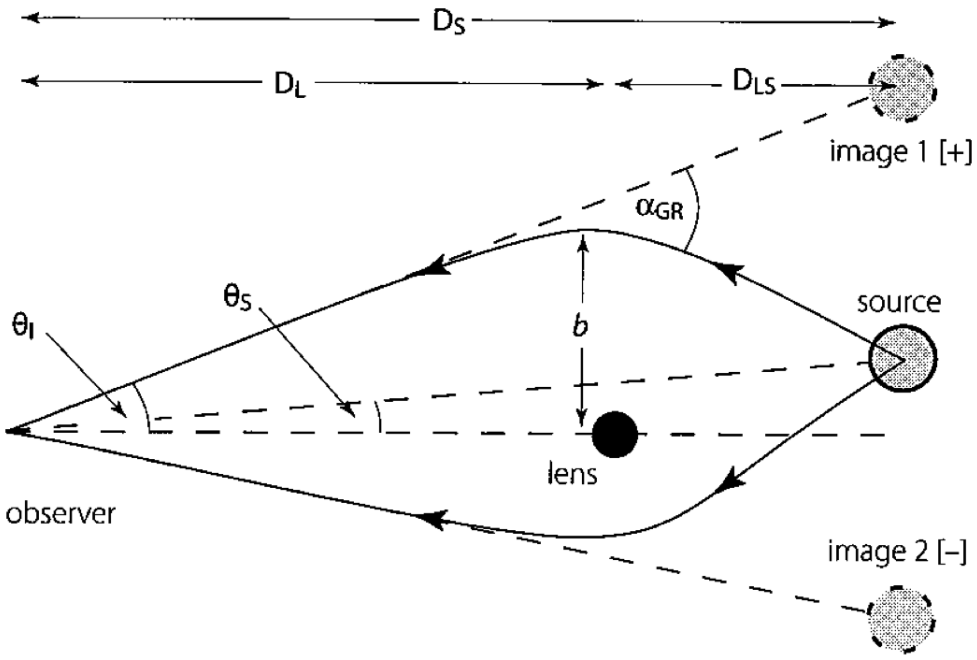

Figure 12: A simplistic view of gravitational lensing. The various quantities are explained in the text. Picture taken from Perryman (2010).

- Its sensitivity bias for lenses halfway to the source, meaning ∼4 kpc if staring at the galactic bulge. This regrettably implies that other detection techniques will have a very hard time doing follow-up observations with the instruments available today.

2.5.1 Some lensing basics

Figure 12 exhibits the relevant ingredients in a simple type of lensing situation. To make sense of the various angles, we start with the *deflection angle* α_{GR}. It is the angle through which light rays from the source is deflected in order to reach the observer. With given lens mass $M_L$and impact parameter b, the deflection angle can be expressed as (Will, 1993)

$$\alpha_{GR} = \frac{4GM_L}{c^2 b}, \tag{2.4}$$

where G is the gravitational constant and c is the speed of light. Noting that the Schwarzschild radius R_S is equal to $^{2GM_L}/_{c^2}$, the expression for eq. 2.4 can be simplified into

$$\alpha_{GR} = \frac{2R_S}{b}.$$

These last two equations are valid approximations when the lens' Schwarzschild radius is negligible in relation to the impact parameter, i.e. $b \gg R_S$.

The remaining angles θ_S and θ_I are respectively the angle between lens and source, and between lens and source image as seen by the observer. The corresponding distances between observer and lens and source are D_L and D_S respectively, with $D_{LS} = D_S - D_L$. We wish to express the image angle θ_I to examine the prospect of resolving the picture. To reach this goal, we start by noting

$$\theta_S D_S = \theta_I D_S - \alpha D_{LS}$$

$$\Leftrightarrow \theta_S = \theta_I - \frac{\alpha D_{LS}}{D_S} = \theta_I - \frac{2R_S D_{LS}}{D_S b} = \theta_I - \frac{2R_S D_{LS} D_L}{D_S D_L b} = \theta_I - \frac{2R_S D_{LS}}{D_S D_L}\frac{1}{\theta_I}$$

$$\Leftrightarrow \theta_I^2 - \theta_I \theta_S - \frac{2R_S D_{LS}}{D_S D_L} = 0. \tag{2.5}$$

This equation is obviously quadratic with respect to the image angle, and so far the model is consistent with observations (we observe two images). For convenience, we now define the *Einstein radius* $\theta_E \equiv \sqrt{2R_S \frac{D_{LS}}{D_L D_S}}$. This permits a simplification of eq.2.5 into

$$\theta_I^2 - \theta_I \theta_S - \theta_E^2 = 0,$$

with solutions

$$\theta_I^+ = \frac{1}{2}\left(\theta_S + \sqrt{\theta_S^2 + 4\theta_E^2}\right),$$

$$\theta_I^- = \frac{1}{2}\left(\theta_S - \sqrt{\theta_S^2 + 4\theta_E^2}\right).$$

The angular separation between the images is thus $\Delta\theta_I = \sqrt{\theta_S^2 + 4\theta_E^2}$. As the source angle is small, we could assume it to be zero[15] and obtain a rough estimation of a typical resolution requirement:

$$\Delta\theta_I \sim \theta_E = \sqrt{2R_S \frac{D_{LS}}{D_L D_S}} \sim 1 \text{ mas},$$

assuming a lens situated half-way to the galactic bulge with a mass of about the sun and a source at around 8 kpc i.e. the galactic bulge. 1 mas is far beyond the capabilities of all but the best ground-based telescopes, meaning the microlensing is mainly observable through its magnification effect.

2.5.2 Magnification

Gravitational lenses do not deflect all rays equally, as a direct consequence of that gravity follows an inverse square law. This will introduce asymmetries in the source wavefronts, with areas of both higher and lower flux than had been

[15] If it actually was zero, the geometry becomes symmetrical and the two images instead become an *Einstein ring*. These are extremely rare but have actually been observed.

observed without a lens present. In the case of higher flux, the magnification can be quantified as the ratio between the image area and the source area (because gravitational lensing does not alter surface brightness of the source. See Schneider et al 1992, section 5.2). The magnification stems from the fact that a larger fraction of the source surface radiates in the direction of the observer.

Assuming a point mass lens and introducing $u = {}^{\theta_S}/_{\theta_E}$, the magnification due to both images may be written

$$A = \frac{u^2 + 2}{u\sqrt{u^2 + 4}},$$

where a quick look reveals that

$$\begin{cases} A \to \frac{1}{u} & \text{if } u \ll 1 \\ A \to 0 & \text{if } u \gg 1 \end{cases},$$

which is not a disaster. The limit $u \to 0$ (which would lead to infinite magnification) is not useful since the model is simplistic both in its geometry and the assumption that the lens is a point etc. Magnification values have been observed to frequently reach 10^2 and even 10^3 i.e. a magnitude increase of between 5 and 10, which is considerable to say the least.

The magnification is one of the observables during a microlensing event. Another observable is the duration of the event. Together with the shape of the event light curve, several physical parameters e.g. the mass ratios and linear separations between lens components and more can be deduced from complex modelling and subsequent least squares fitting. See Gould et al. (2006b) for details on this.

2.6 Direct observation

A direct observation means capturing the point-spread function of the exoplanet on e.g. a CCD, regardless of if the light is reflected from the parent star or thermally emitted from the planet itself. Resolving exoplanets also counts, obviously, but that is a prospect far into the future. There is nothing in principle that prevents a CCD or some other detector from revealing the presence of exoplanets directly, but the practicalities are of dominant concern - today this technique only discovers the larger type of Jovian planets, preferably with reflecting ring systems (for extra brightness if the spatial alignments are favourable).

Of what nature are these mentioned practicalities? Many different kinds, it turns out.

- Angular separation is a function of distance. Beyond a certain minimum distance, resolving the planet from its star is science fiction from where we stand today.
- Noise. Stars are often between 10^5 and 10^{10} times brighter than their planets, depending on albedo and a few other things. The signal-to-noise ratio of the starlight will overpower the exoplanet signal significantly.

- The costs for building telescopes of adequate size are ludicrous - the E-ELT is estimated to cost a little more than €10^9. This disadvantage can be expected to grow less painful as construction technologies are optimized and resources are amassed at increasing rates.

The first problem is not really solvable in and of itself (unless someone is psyched to embark on a very, very, very long odyssey). All you can do is build bigger and better telescopes, with consequences mentioned in point three. The second problem is where most of today's creative resources are focused - many different methods, each aiming to completely or to a sufficient degree eliminate the parent star signal, are being invented, developed, improved and tested. The older of these methods are hubbed around a simple piece of opaque material placed in front of the star PSF[16], introducing diffraction effects and such undesirables. Newer methods turn to the quantum world, exploiting properties of light with complex contraptions, finding various ways of creating self-interference in hopes of eliminating starlight while keeping as much light as possible from nearby (fainter) sources. The various branches of this field collectively constitute *coronagraphy*, since the basic idea was first employed in an attempt to observe the solar corona (which is a million times fainter than the photosphere).

2.6.1 Types of coronagraphy

There are many kinds of different approaches to neglect the star signal while keeping the planet signal as intact as possible. Here follows very brief outlines of some of them.

Lyot coronagraphs are the conceptually simplest kind. As the image is focused in the focal plane, a physical object is placed so as to absorb or reflect the light that happens to cross its path, leaving only off-axis structure plus some diffraction effects from the on-axis blocking. A Lyot stop is employed in an attempt to block out the remaining diffraction effects.

Interferometric coronagraphs exploit the self-interference of light. Incoming light is by means of various mechanisms split into two or more identical parts as it enters the telescope pupil. The phase of the separated beams of light are then somehow manipulated and upon fusing the beams afterwards, destructive interference selectively removes undesirable light sources.

Apodisation coronagraphs use amplitude or phase masks to suppress parts of the image, i.e. they manipulate point-spread-functions that if present would prevent the contrast levels necessary to see dark objects like planets. Amplitude masks are reminiscent of the Lyot approach, but offer greater flexibility and detail in the physical blocking of the light. Phase masks utilize destructive interference for similar effect.

Improved Lyot coronagraphs replace the classical componenths of a Lyot coronagraph with either amplitude masks or phase masks to allow for a more flexible and finer approach when reducing diffraction. Examples of improved

[16]Point-Spread-Function: The distribution of intensity in an unresolved picture of for example a distant star or quasar.

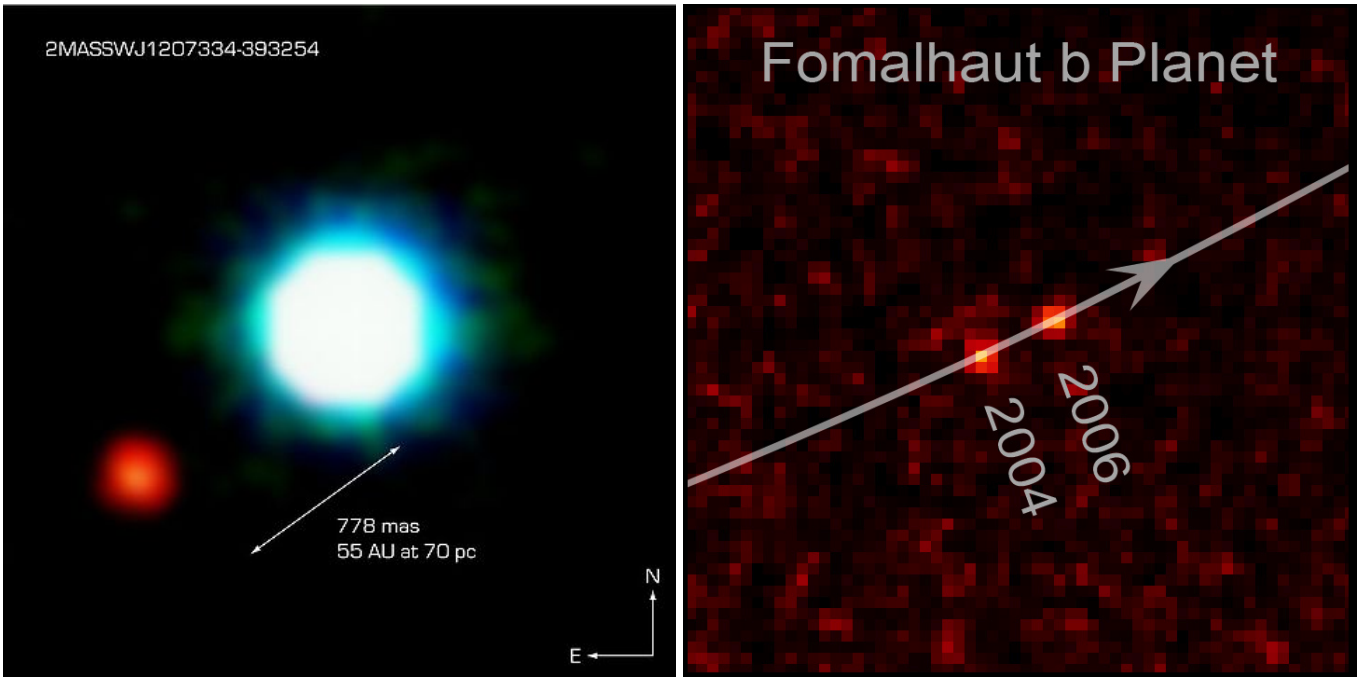

Figure 13: The very hot and massive planet 2M1207b directly imaged alongside its brown dwarf parent (left), and two snapshots of the planet Fomalhaut b in its huge orbit around its parent star (right).

Lyot coronagraps include the *optical vortex coronagraph* and the *four-quadrant phase mask*.

Additional approaches include e.g. *Pupil replication* (Greenway et al., 2005), *Pupil filtering/remapping* (Perrin, 2006) and *Free-flying occulters*. Free-flying occulters are self-descriptive - man-made objects intended for positioning between a star and the observing telescope. Several proposals on free-flying occulters have been made e.g. Schultz et al., (2003); Copi & Starkman (2000) and Cash et al. (2005).

3 The final step - the least-squares algorithm

In this thesis, the detection methods from radial velocity and astrometry have been given extra detail, but as the reader might have noticed, the sections above are missing a crucial part: How do we combine model and measurements into actual estimates of the physical parameters we are seeking to find?

The answer is for most problems of this sort a numerical least-squares algorithm. These algorithms take data from measurements as input, and then output the model parameters that best fit the data put in. The models of exoplanet systems in this thesis are largely non-linear with respect to their various parameters, which obviously must be taken into account in the algorithm.

3.1 The basic idea

The method of least squares dates back to Gauss and his work during the final years of the 18th century and the first few of the 19th. It is an algorithm that seeks to minimize the effect of measurement error on the physical model you're trying to find. The conceptually simplest way of describing the fundamental idea goes something like:

1. Choose some model f describing the sought after quantity in terms of some independent variable y (the number of independent variables is not constrained in principle) and a set of unknown parameters $\mathbf{x} = (x_1, x_2, x_3, ...)$: $f = f(y, \mathbf{x})$.

2. Measure the sought after quantity as a function of the independent variable and express the result as a data set $(f_1, y_1); (f_2, y_2); (f_3, y_3) ... = (f_i, y_i)$.[17]

3. Define a new function through $r_i = f(y_i, \mathbf{x}) - f_i$: r_i is the quantity value mismatch between your model's prediction $f(y_i, \mathbf{x})$ and the measured value f_i.

4. Define another function through $S = r_1^2 + r_2^2 + r_3^2 + ... = \sum r_i^2$: S is the sum of all the squares of the mismatches between model and measurement.

[17] Step 1 and step 2 can of course be performed in any order.

5. We wish to find the set of parameters $\mathbf{x}$ that makes S as small as possible (in other words, find the best possible model for the data set obtained), so we observe that S is an analytical function and remember from high school how the minima (extrema) of such functions are found - the derivative is zero. So we form the following system of equations[18]:

$$\begin{aligned} \frac{\partial S}{\partial x_1} &= 0 \\ \frac{\partial S}{\partial x_2} &= 0 \\ \frac{\partial S}{\partial x_3} &= 0 \\ \frac{\partial S}{\partial x_4} &= 0 \\ &\vdots \end{aligned} \tag{3.1}$$

6. Solve for the parameters and calculate. When you've found the $\mathbf{x}$ that solves the above equations simultaneously, you've found the best model[19] and are done.

3.2 However...

If it looks simple, you're not looking deep enough. In the introduction, some steps are far from trivial. What if the elements of $\mathbf{x}$ cannot be analytically solved for? This is an example of where a simple idea turns complicated when you want to apply it on the real world.

When the elements of $\mathbf{x}$ appear as non-linear functions, the method used is renamed into the fabulous 'non-linear least-squares'. This algorithm can take many forms in practice. A few examples include Levenberg-Marquardt, Nelder-Mead, Davidon-Fletcher-Powell and Gauss-Newton. The essence of the concept remains the same, but some re-thinking is necessary.

For starters, the zero-derivative approach is no longer a means of finding the elements in $\mathbf{x}$, even though the solution to the set of equations above is still what we're looking for. What to do instead? Most, if not all, algorithms start off by guessing a $\mathbf{x}$, either based on previous estimates or on nothing. The implications and/or results of this guess is then analyzed and turned into a (hopefully) better guess, until subsequent guesses are practically identical i.e. the minimum of S has been reached. The actual steps taken vary from algorithm to algorithm. Indeed, some algorithms simply guess all over the place, and are of course not suitable for great accuracy. Instead, they could be used to find a decent first guess for more sophisticated algorithms.

[18] If you solve for the parameters from these equations, you may call the new but equivalent equations *normal equations*.

[19] In the sense that the function S is minimized.

I find examples the most accesible way of introducing new concepts and ideas, and as Newton's method (on which the Gauss-Newton method may be regarded an improvement) is to the best of my knowledge the simplest non-linear least squares algorithm, it will have to do as an introductory example:

1. Having expressed the derivatives of S with respect to its parameters, guess an initial set of parameters $\mathbf{x}_i$.

2. Express $\frac{\partial^2 S(\mathbf{x}_i)}{\partial \mathbf{x}^2}$ as the slope of the tangent to the point $\left(\frac{\partial S(\mathbf{x}_i)}{\partial \mathbf{x}}, \mathbf{x}_i\right)$: $\frac{\partial^2 S}{\partial \mathbf{x}^2} = \frac{\Delta \frac{\partial S}{\partial \mathbf{x}}}{\Delta \mathbf{x}} = \frac{\frac{\partial S}{\partial \mathbf{x}} - 0}{\mathbf{x}_i - \mathbf{x}_{i+1}}$.

3. Solve for the linear root: $\mathbf{x}_{i+1} = \mathbf{x}_i - \frac{\frac{\partial S}{\partial \mathbf{x}}}{\frac{\partial^2 S}{\partial \mathbf{x}^2}}$.

Describing it in words, it's best to imagine the derivatives of S as a function in parameter space of $\mathbf{x}$ dimensions. The first guess corresponds to a point somewhere on the curve $\frac{\partial S}{\partial \mathbf{x}}$, and from this point we draw its tangent all the way down or up to the line corresponding to $\frac{\partial S}{\partial \mathbf{x}} = 0$ i.e. the zero-level. This is basically a linearization of $\frac{\partial S}{\partial \mathbf{x}}$ in the point specified by the initial guess. The slope of this linear approximation can be expressed using the two points now available, and $\mathbf{x}$ at the zero-level is now your new guess. Picture 14 might help to clear things up.

Note that in Newton's method, the second derivative of S must be available in a closed analytical form. This requirement does not appear in all methods. For example, the Levenberg-Marquardt algorithm used by Howard&Wright (2009) only requires analytical forms of the first derivative.

3.3 Matrix form

The system of equations 3.1 can be condensed into a single matrix equation. This comes in handy when the numerical problem is large - if your data set is huge, or the number of parameters is large (which is the case when fitting data to a model that accounts for multiple planets, for example). A commonly used form for the normal equations is

$$\mathbf{A^T A \Delta x} = \mathbf{A^T r},$$

where $\mathbf{r}$ is the set of *residuals*: $\mathbf{r} = (r_1, r_2, r_3, ...)$, $\mathbf{\Delta x}$ is the *correction*, i.e. the difference between the upcoming estimate and the previous one: $\mathbf{\Delta x} = \mathbf{x}_{i+1} - \mathbf{x}_i$ and $\mathbf{A}$, the *observation matrix*, is the Jacobian of $\mathbf{r}$: $\mathbf{A} = \begin{bmatrix} \frac{\partial r_1}{\partial x_1} & \frac{\partial r_1}{\partial x_2} & \cdots \\ \frac{\partial r_2}{\partial x_1} & \frac{\partial r_2}{\partial x_2} & \cdots \\ \vdots & \vdots & \ddots \end{bmatrix}$.
Solving for the correction, which must be done to find the new guesstimate of $\mathbf{x}$, you get:

$$\mathbf{\Delta x} = \left(\mathbf{A^T A}\right)^{-1} \mathbf{A^T r}.$$

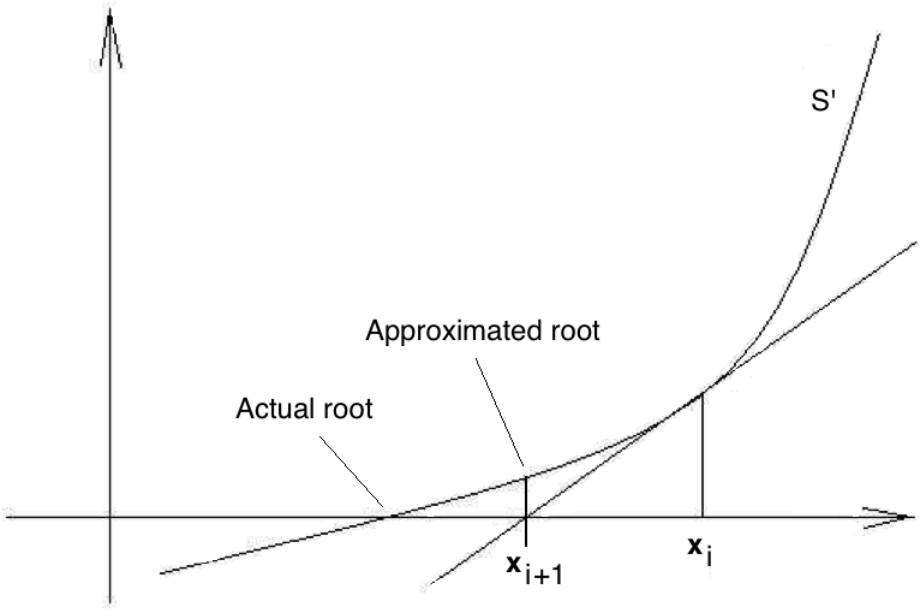

Figure 14: The Newton algorithm in a nutshell. $\mathbf{x_i}$ is the initial guess. Note how the algorithm will never find anything but the closest root, which might not correspond to the global minimum of S.

Often, this equation is condensed further into

$$\mathbf{\Delta x} = \mathbf{N}^{-1}\mathbf{b},$$

where then $\mathbf{N} = \mathbf{A^T A}$ and $\mathbf{b} = \mathbf{A^T r}$.

Example techniques and algorithms that may be employed to solve this equation include Cholesky decomposition and Householder's methods. Generally, $\mathbf{\Delta x}$ or $\mathbf{b}$ will never reach zero no matter how perfect the algorithm, because of measurement errors and the fact that the model used is probably not completely realistic.

4 Combining astrometric and radial velocity data

This thesis ends with a briefly outlined suggestion on how to use radial velocity data for improvement of astrometric detection of exoplanets. Currently, the radial velocity technique is the mainstream in exoplanet detection, with greater success than any other technique. It has a serious intrinsic flaw however, and that is its $m \sin i$ degeneracy - without help from other techniques, you obtain but a minimum mass of the planet. Astrometry has the potential to save the day, as it will be able to provide all seven orbital parameters, including the inclination i. As a bonus, it can also constrain the exoplanet mass and relative inclinations in multiplanet systems. Its success so far has been very limited due to the high demands on instrument accuracy.

Astrometry is currently undergoing a renaissance through the global space astrometry mission Gaia which will amass direct astrometric data on about 1 billion sources between magnitudes 6 and 20, along with some indirect data on exoplanets of Jupiter mass. Additional astrometric missions continue to be proposed (examples include SIM and NEAT), and they aim to detect exoplanets with Earth-like mass in addition to the basic astrometry. Radial velocity measurements for the detected astrometric planets are either already available, or obtainable through follow-up surveys.

The strengths of combining these two detection methods are evident in that astrometric measurements cannot distinguish the ascending node from the descending node. Radial velocity can (see Catanzarite, 2010). Additionally, as four of the orbital elements (Ω, ω, i, a_*) are present in both the astrometric and radial velocity solution, this will constrain the 3-D orbit with superior accuracy and precision because the parameters of an orbit fitted with both radial velocity and astrometric data sets must be consistent with both.

Catanzarite (2010) and Wright & Howard (2009) have both proposed methods of combining radial velocity and astrometric data. Catanzarite (2010) has focused on minimizing the number of parameters involved, hoping to improve computational speed. However, this process requires a complex and iterative post-processing phase to ensure that the data sets are consistent. Wright & Howard (2009) have used a more conventional approach.

The astrometric solution can be partially linearized by using the Thiele-Innes constants explained in an earlier section. The three nonlinear parameters e, t_p

and P remain nonlinear, however. For an N-planet system then, the astrometric solution is modeled with $6 + 7N$ parameters[20], $3N$ of which are the nonlinear ones just mentioned. For the radial velocity solution a similar linearization can be performed. Each planet then has the basic nonlinear parameters (e, t_p, P), two linear parameters C and H (see Wright & Howard (2009) for details on these) and an offset γ. All of these together result in a total of $7 + 9N$ parameters, of which two per planet are redundant. This redundancy does not cause much harm and will, for simplicity's sake, be duly ignored.

4.1 Least-squares incorporation

The scheme above will be developed for the Gaia mission in the coming years. Translating into mathematics of the least-squares method will be unavoidable sooner or later, so here follows an introduction on how this translation might look like. First, one must specify how to set up the normal equations. The Gaia data processing uses normal equations constructed on the fly by summing the contributions from a large number of observation equations. The individual observation equations can be written (cf. equations in section 3.3):

$$\mathbf{A}_{m,n}\mathbf{\Delta x}_n = \mathbf{r}_m,$$

where the matrix $\mathbf{A}$ has dimensions $m \times n$, with the rows $m \gg n$ corresponding to individual observation equations. $\mathbf{\Delta x}$ with length n is the (column) vector of parameter corrections (or 'updates') and $\mathbf{r}$ is the residual (column) vector of length m. In practice, we do not have to keep track of these quantities. Instead they can be added directly to form a set of normal equation, given by

$$\mathbf{A^T A \Delta x} = \mathbf{A^T r},$$

which in shorthand notation is, as in the previous section,

$$\mathbf{N \Delta x} = \mathbf{b}.$$

This equation can be solved by either a linear or nonlinear factorization algorithm. In a combined radial velocity and astrometric solution, the only introduced complication is defining the construction of the individual rows of observation. We do this with two types of rows corresponding to the two types of observational data as illustrated below

[20] Normally we only solve for 5 astrometric parameters, but in some cases we can also solve for radial motion.

$$
\begin{bmatrix}
-\frac{\partial R_1}{\partial \alpha} & -\frac{\partial R_1}{\partial \delta} & -\frac{\partial R_1}{\partial \varpi} & -\frac{\partial R_1}{\partial \mu_{\alpha\star}} & -\frac{\partial R_1}{\partial \mu_\delta} & -\frac{\partial R_1}{\partial \mu_r} & 0 & \\
0 & 0 & 0 & 0 & 0 & -\frac{\partial R_2}{\partial v_r} & -\frac{\partial R_2}{\partial \gamma} & \cdots \\
\vdots & \vdots & \vdots & \vdots & \vdots & \vdots & \vdots &
\end{bmatrix}
$$

$$
\cdots \quad
\begin{bmatrix}
-\frac{\partial R_1}{\partial A} & -\frac{\partial R_1}{\partial B} & -\frac{\partial R_1}{\partial F} & -\frac{\partial R_1}{\partial G} & 0 & 0 & -\frac{\partial R_1}{\partial e} & -\frac{\partial R_1}{\partial t_p} & -\frac{\partial R_1}{\partial P} \\
0 & 0 & 0 & 0 & -\frac{\partial R_2}{\partial C} & -\frac{\partial R_2}{\partial H} & -\frac{\partial R_2}{\partial e} & -\frac{\partial R_2}{\partial t_p} & -\frac{\partial R_2}{\partial P} \\
\vdots & \vdots & \vdots & \vdots & \vdots & \vdots & \vdots & \vdots & \vdots
\end{bmatrix} \times
$$

$$
\times
\begin{bmatrix}
\Delta\alpha \\ \Delta\delta \\ \Delta\varpi \\ \Delta\mu_{\alpha\star} \\ \Delta\mu_\delta \\ \Delta\mu_r \\ \Delta\gamma \\ \Delta A \\ \Delta B \\ \Delta F \\ \Delta G \\ \Delta C \\ \Delta H \\ \Delta e \\ \Delta t_p \\ \Delta P
\end{bmatrix}
=
\begin{bmatrix}
R_1 \\ R_2 \\ \vdots
\end{bmatrix}
$$

This huge equation demonstrates how two rows of observations, one astrometric (upper) and one radial velocity (lower), could be combined into the observation matrix. The vertical suspension points indicate that an additional row (ideally one from astrometry and one from radial velocity) will be added for each data point, while the zeroes indicate that no information on the corresponding parameter is available from this observation (the horizontal suspension points are simply there to remedy limitations on page formatting). Complications will arise as entries for e, T and P are nonlinear, but the equation is sufficient for outlining the principle. The sixth column in $\mathbf{A}$ appears at first glance not well-formed, but radial velocity and radial motion are closely (mathematically) related and thus conceptually equivalent in this outlined idea. For a multiplanet fit, you would for every additional planet add nine columns to $\mathbf{A}$ and nine rows to $\mathbf{\Delta x}$.

A joint solution such as this for Gaia or similar missions could help to better constrain the physical parameters of the observed stars and thus their planets. Gaia is presently due for launch in 2013.

5 Conclusion

On page 4 in Perryman's *The Exoplanet Handbook* from 2011, you can find figure 15. The anticipated progress is a bit dated, since it was taken from a paper by Perryman in 2000.

Some comments on the various methods with regard to Perryman's chart:

Timing

The strength of the timing method is millisecond pulsars, the strength of which Perryman did not realize as he made the picture. As mentioned earlier in the thesis, planets down to 0.02 Earth masses can be detected if they orbit millisecond pulsars. No other technique can presently accomplish this. Apart from the millisecond pulsars however, the timing method does not hold great promise in relation to other techniques. The prerequisites of both small inclinations and a periodic signal of some sort leads me to think that this technique is more of an oppurtunistic approach. For the astrobiologists the timing method is even less interesting since neutron stars, white dwarves and pulsating stars are all implying a violent environment for any potential life-bearing planet. Eclipsing binaries would be the exception to this, but their rarity and sluggish signal periods are unavoidable problems.

Radial Velocity

Radial velocity has been a cornerstone for exoplanet detection since its early days, and there's no reason it should not remain highly relevant and applicable. It should never face complete obsoleteness when bearing in mind that it does not depend too much on distance, and that it's a necessary complement to the transit method. Perryman's extrapolation of its capabilities seem reasonable.

Astrometry

This is another instance where Perryman is rather pessimistic. Astrometry is in theory very powerful - it constrains many parameters, and does not suffer from the presence of multiple planets. The only major drawback would be its dependence on distance. If any of the mission proposals on searching for exoplanets through astrometry (e.g. NEAT and SIM) launches, then Earth-mass planets not too far from here might very well be detectable. It is hard to tell when to expect this to happen though. Perryman's projection is a cointoss.

Microlensing

The microlensing method is a little bit odd and exotic in relation to other techniques. It can detect planets at extremely large distances, with a peak sensitivity to planets inside the habitable zones of most main-sequence stars, but lensing incidents are rare and difficult to complement with other techniques. Perryman's projection of the photometric performance is probably rather reasonable

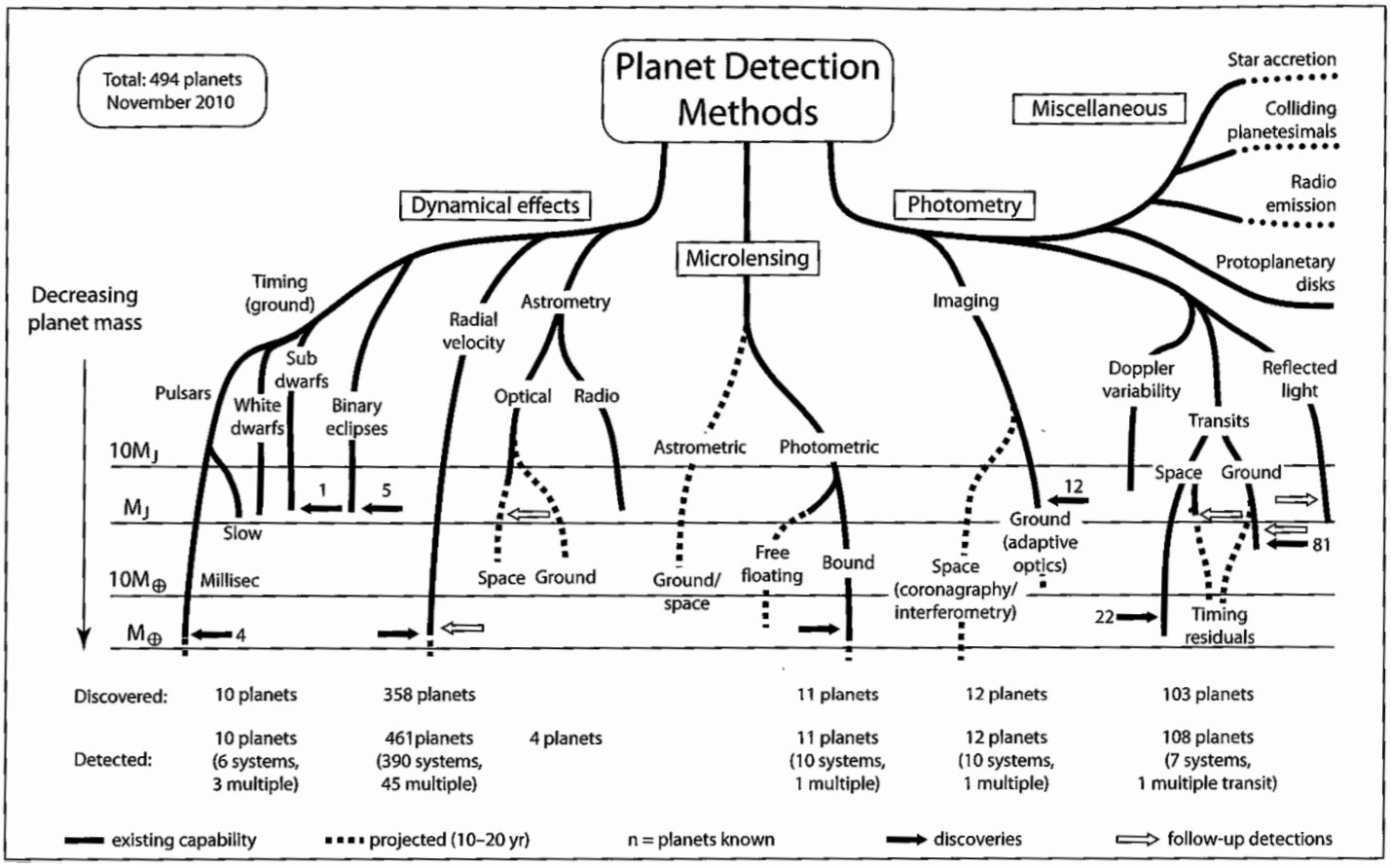

Figure 15: Perryman's chart of detection methods and their projected capabilities.

as the lensing effect is not a strong function of planet mass. The prospect of detecting astrometric effects from lensing is, like pure astrometry, slumbering until Gaia or instruments of comparable resolution are operational, but may very well develop into another functional opportunistic approach.

Direct imaging

The Earth's atmosphere is a major problem for direct imaging. Building the required huge telescopes is preferably done on ground level for practical and economical reasons, but then you need adaptive optics of extreme complexity which might still not be enough to reach necessary resolutions. A 100 m class space telescope would be a dream come true for many astronomers, but is presently sci-fi. There is promise however in coronagraphy. If good progress is made in this field and then applied at space-based observatories, Perryman could well be correct in his projection.

Transits/Photometry

The transit method has both major drawbacks and major advantages. Its weakness revolves around its dependency on minute inclinations and ambigious data (sunspots etc.), while it is strong in parameter extraction and compatibility with survey-type missions eg. Kepler. If photometric sensitivity progresses unpredictably well in the future, the reflected light from planets may become a new cornerstone in exoplanet detection, as the inclination requirement is softened up slightly (in principle, anything but head-on orbits could be analyzed by modulations of the reflected light due to phases). I can't help but think that Perryman is a bit on the pessimistic side regarding reflected light, and I don't see why he would project stagnation for both ground- and space-based photometry. I see great promise in the transit method, provided higher photometric sensivity.

References

[1] Perryman, MAC, 2011, *The Exoplanet Handbook*. Cambridge University Press.

[2] -, 2000, Extra-solar planets. *Reports on Progress in Physics,* **63**, 1209-1272.

[3] Wright JT, Howard AW, 2009, Efficient fitting of multiplanet keplerian models to radial velocity and astrometry data. *ApJS*, **182**, 205-215.

[4] Mandel K, Agol E, 2002, Analytic light curves for planetary transit searches. *ApJ*, **580**, L171-L175.

[5] Seager S, Mallén-Ornelas G, 2003, A unique solution of planet and star parameters from an extrasolar planet transit light curve. *ApJ*, **585**, 1038-1055.

[6] Barnes JW, 2007, Effects of orbital eccentricity on extrasolar planet transit detectability and light curves. *PASP*, **119**, 986-993.

[7] Kipping, 2008, Transiting planets: light-curve analysis for eccentric orbits. *MNRAS*, **389**, 1383-1390.

[8] Collier Cameron AC, Horne K, Penny A, et al., 1999, Probable detecetion of starlight relfected from the giant planet orbiting τ Boo. *Nature,* **402**, 751-755.

[9] Leigh C, Collier Cameron A, Guillot T, 2003a, Prospects for spectroscopic refleced-light planet searches. *MNRAS*, **346**, 890-896.

[10] Seidelmann PK, 1992, *Explanatory Supplement to the Astronomical Almanac.* University Science Books, New York.

[11] Green RM, 1985, *Spherical Astronomy.* Cambridge University Press.

[12] Will CM, 1993, *Theory and Experiment in Gravitational Physics.* Cambridge Universty Press, Second Edition.

[13] Gould A, Udalski A, An D, et al., 2006b, Microlens OGLE-2005-BLG-169 implies that cool Neptune-like planets are common. *ApJ,* **644**, L37-L40.

[14] Leroy J, 2000, *Polarisation of Light and Astronomical Observation.* Gordon and Breach, Amsterdam.

[15] Carciofi AC, Magalhães AM, 2005, The polarisation signature of extrasolar planet transiting cool dwarfs. *ApJ,* **635**, 570-577.

[16] Seager S, Deming D, Valenti JA, 2009, Transiting exoplanets with JWST. *Astrophysics in the Next Decade, Astrophysics and Space Science Proceedings,* 123-130.

[17] Schneider P, Ehlers J, Falco EE, 1999, *Gravitational lenses.* Springer.

[18] Catanzarite JH, 2010, A new algorithm for fitting orbits of multiple-planet systems to combined RV and astrometric data, *eprint arXiv:*1008.3416.

[19] Greenaway AH, Spaan FHP, Moruai V, 2005, Pupil replication for exoplanet imaging. *ApJ*, **618**, L165-L165.

[20] Perrin G, Lacour S, Woillez J, et al., 2006, High dynamic range imaging by pupil single-mode filtering and remapping. *MNRAS*, **373**, 747-751.

[21] Schultz AB, Jordan IJ, Kochte M, et al., 2003, UMBRAS: a matched occulter and telescope for imaging extrasolar planets. *SPIE Conf Ser,* volume **4860**, 54-61.

[22] Copi CJ, Starkman GD, 2000, The Big Occulting Steerable Satellite (BOSS). *ApJ*, **532**, 581-592.

[23] Cash W, Kasdin J, Seager S, et al., 2005, Direct studies of exoplanets with the New Worlds Observer. *SPIE Conf Ser,* volume **5899**, 274-285.